

POVERTY, INFECTIONS DISEASE CONTROL, AND EXTERNALITIES IN
RURAL ECONOMIES

A Thesis

Presented to the Faculty of the Graduate School
of Cornell University

In Partial Fulfillment of the Requirements for the Degree of
Master of Science

by

Molly Jane Doruska
December 2022

© 2022 Molly Jane Doruska

ABSTRACT

Infectious disease exposure often covaries with labor productivity and incomes in ways that can trap people in a cycle of ill health and poverty. We explicitly model the interaction between agricultural households and their natural environment using a bioeconomic model of schistosomiasis infection in northern Senegal. We explore this relationship in the context of aquatic vegetation removal, an ecological intervention designed to decrease schistosomiasis infection by disrupting the life cycle of the parasite. We find evidence of a poverty-disease trap as incomes are lower when households do not remove vegetation, as is true presently. Vegetation removal decreases infection relative to the no removal case. Eliminating the feedback loop between fertilizer and vegetation growth allows households to fully clear the water source and results in higher labor productivity and incomes. The results underscore the importance of fully addressing the cycle of infection when working to reduce disease burdens and poverty.

BIOGRAPHICAL SKETCH

Molly Doruska was born in Iowa. She earned a Bachelor of Arts in Economics and French and Francophone Studies from Lawrence University in Appleton, Wisconsin. While at Lawrence, she participated in the Francophone Seminar in Dakar, Senegal where she studied at the Baobab Center in Dakar. She also interned at the World Food Prize Foundation in Des Moines, Iowa prior to finishing her studies at Lawrence. While at the Charles H. Dyson School of Applied Economics and Management, she led a five-week pilot study in agricultural villages with water access points in the Saint Louis and Louga regions in Senegal. She will continue as a PhD student at the Charles H. Dyson School of Applied Economics and Management with research interests in development, environment, and resource economics.

ACKNOWLEDGMENTS

I would like to express my deepest gratitude to Chris Barrett for his kind guidance and support throughout this project. He was instrumental in helping me develop the ideas within and troubleshoot the many problems that arose throughout the project.

I am extremely grateful to Brian Dillon for helping me further develop my ideas and find the bigger picture throughout this project.

I am also thankful to Jason Rohr for kindly explaining much of the disease ecology of schistosomiasis to me and for sharing the data collected by his team that made this project possible. I also would like to thank Chris Haggerty and Alex Sack for answering countless questions about the data collected in Senegal.

I am also grateful for the guidance of Alex Perkins and Sean Moore whose guidance allowed me to develop and calibrate the disease ecology submodel of schistosomiasis.

I would like to extend my sincere thanks to Ivan Rudik who provided countless helpful insights into the optimization in this project and who pushed me to start developing this project in his class.

Special thanks to Shanjun Li for offering comments and suggestions throughout the project and always pushing me to further develop all aspects of the project.

Many thanks to Kira Lancker for her kind and sage advice throughout the project and for always being willing to read and comment on the project.

I would also like to thank Nicolas Jounard, Momy Seck, and the team at SIA for all of their data collection efforts that made this project possible and for being so welcoming during my visit to Senegal.

I had the pleasure of working closely with Daouda Thaim in Senegal and he was instrumental in helping me better understand the context of my study. I would also like to thank Chiekh Oumar Diaw for his help in collecting data during the field visit related to this project.

This project greatly benefited from comments from seminar participants in AEM 7650 and AEM 7151 and Leo Borja, Tarana Chauhan, Natasha Jha, Tess Lallemand, Aleks Michuda, Ben Norton, Sergio Puerto, Vanisha Sharma, and Dana Smith during work group meetings.

This endeavor would not have been possible without the funding of the National Science Foundation (NSF) and the National Institutes of Health (NIH).

Finally, I would like to thank Alec Timpe for always answering my questions about science and helping me think through countless problems. I am eternally grateful for your excitement about this project that motivated me to find answers even when it was difficult.

TABLE OF CONTENTS

ABSTRACT	ii
BIOGRAPHICAL SKETCH	iii
ACKNOWLEDGMENTS	iv
TABLE OF CONTENTS	vi
LIST OF FIGURES	viii
LIST OF TABLES	ix
INTRODUCTION	1
LITERATURE AND CONTEXT	6
2.1 Poverty-Disease Traps	6
2.2 The Senegalese Context	8
2.3 Aquatic Vegetation Removal	10
BIOECONOMIC MODEL	12
3.1 The Household's Problem	12
3.2 Disease Ecology Model for Schistosomiasis	22
3.3 Linking the Two Submodels	27
HOUSEHOLD SIMULATIONS	30
4.1 Simulations with No Vegetation Harvest	31
4.2 Simulations with Vegetation Harvest	33
4.3 Simulations with Vegetation Harvest and No Fertilizer Effect	36
DISCUSSION AND CONCLUSION	40
Appendix A: Harvested Vegetation Production	44
Appendix B: Disease Ecology Submodel Parameterization	45
B.1 Modifications	46
B.2 Simulations	49

LIST OF FIGURES

Figure 4.1 Median Labor Availability and Labor Allocation Shares for Simulations without Vegetation Harvest	32
Figure 4.2 Median Fertilizer Use, Income, Household Infection Rate, and Vegetation Load for Simulations without Vegetation Harvest	33
Figure 4.3 Median Labor Availability and Labor Allocation Shares for Simulations with Vegetation Harvest	35
Figure 4.4 Median Fertilizer Use, Income, Household Infection Rate, and Vegetation Load for Simulations with Vegetation Harvest	36
Figure 4.5 Median Labor Availability and Labor Allocation Shares for Simulations with Vegetation Harvest and No Fertilizer Effect	38
Figure 4.6 Median Fertilizer Use, Income, Household Infection Rate, and Vegetation Load for Simulations with Vegetation Harvest and No Fertilizer Effect	39
Figure B.1 Five-Year Continuous Time Simulation Results	50

LIST OF TABLES

Table 2.1 Summary Statistics of Agricultural Households in the Saint Louis and Louga Regions	10
Table 3.1 Estimated Expenditure Shares	18
Table 3.2 Estimated Factor Cost Shares	19
Table 3.3 Parameters for the Household Model	21
Table 3.4 Parameters for the Disease Ecology Model	26
Table 3.5 Starting Values of Disease Ecology Parameters	27
Table 4.1 Land Endowments for Household Simulations	30
Table A.1 Vegetation Production Function Estimates	44
Table B.1 Parameters for the Disease Ecology Model in Gao et al. (2011)	46
Table B.2 Adjusted Parameters for the Disease Ecology Model	48

CHAPTER 1

INTRODUCTION

The global population is expected to climb to almost 10 billion people with much of this growth occurring in the developing world where there still is widespread poverty and infectious disease (Vollset et al., 2020). Meeting the needs of this growing population requires more intensive agricultural production and this agricultural intensification will likely require increased fertilizer use which can increase disease burdens (Rohr et al., 2019). Thus, poor areas across the developing world face increased risk of poverty-disease traps whereby disease inhibits human capital accumulation and poverty persists (Barrett & Carter, 2013; Barrett et al., 2006; Barrett, Garg, & McBride, 2016; Barrett, Carter & Chavas, 2019; Bonds et al., 2010; Carter & Barrett, 2006; Kraay & McKenzie, 2014; Ngonghala et al., 2014, 2017; Zimmerman & Carter, 2003). Therefore, improving the livelihoods of millions of poor individuals requires understanding the potential feedbacks between poverty, disease, agricultural production, and rural households.

One potential cause of a poverty-disease trap is schistosomiasis, a neglected tropical disease that disproportionately affects children. In addition to the more than 200 million people around the globe that are currently infected, 800 million people are at risk of infection (Steinmann et al., 2006; Gryseels et al., 2006; Hotez et al., 2014). Schistosomiasis is caused by a snail-hosted flatworm. Snails infected with schistosomes inhabit aquatic plants in freshwater habitats (lakes and rivers). These snails release larval schistosomes into the water, which then penetrate the skin while people perform daily activities, like washing clothes or swimming (Stelma et al., 1994;

Haggerty et al., 2020). Adult worms settle in the gastrointestinal (*Schistosoma mansoni*) or urinary (*Schistosoma haematobium*) tract of infected individuals causing a number of ailments including, but not limited to, loss of tissue function, stunted growth, and learning deficits (King, Dickman & Tisch, 2005; Kjetland et al., 2006; Mohammed, Edino & Samaila, 2007). Conventional methods to control schistosomiasis rely on mass deworming, whereby all children and/or adults within a village receive deworming medication to clear current infections. However, mass deworming does not clear snails and schistosomes from the water sources, thus reinfection occurs quickly (Halstead et al., 2018; Liang, Abe & Zhou, 2018). While mass deworming reduces the current level of human infection, reducing long-term cycles of schistosomiasis infection and reinfection requires multiple strategies that target different parts of the infection cycle (Grimes et al., 2015; Hoover, Sokolow, et al., 2020; Liang, Abe & Zhou, 2018).

In this paper, we develop a bioeconomic model to examine the relationship between agricultural production, poverty, and disease in norther Senegal and evaluate the potential of the agroecological intervention of aquatic vegetation removal to break the poverty-disease trap. Aquatic vegetation removal reduces snail habitat, thereby reducing host and worm populations thus lowering infection at the water source and supplementing infection control through deworming. We start with a classic non-separable agricultural household model (Strauss, Squire & Singh, 1986) and connect it to a disease ecology model of schistosomiasis (Gao et al., 2011) through household decisions about aquatic vegetation harvest and investment in human capital through infection status. We inextricably link the economic and disease ecology models in the

spirit of Barrett and Arcese (1998) and Stephens et al. (2012) to directly model the connections between economic decisions and environmental changes. Specifically, we ask under what conditions households undertake aquatic vegetation removal, and under what conditions this vegetation removal is sufficient to control schistosomiasis transmission. We solve this model for household types with different wealth endowments to understand how wealth influences the optimal behavior of households and thus disease, agricultural and household income outcomes.

Our results highlight two key feedback loops faced by households. First, we find evidence supporting the existence of a poverty-disease trap as household incomes remain low when vegetation remains within the water source. When vegetation growth remains unchecked by households, schistosomiasis infections reduce household labor availability reducing the amount of productive time allocated towards agricultural production and decreasing overall incomes. However, when households clear the waterway, infections plummet and productivity and incomes increase.

Second, fertilizer run-off provides key nutrients that can limit the effectiveness of aquatic vegetation removal. In the model, growth from fertilizer run-off sustains the vegetation population and since vegetation grows quickly, this small population induced by fertilizer run-off allows infection to persist. With higher infection levels, households are unable to fully break the cycle and remain trapped at low levels of income and productivity. These simulations highlight that while fertilizer increase agricultural output, it also has the potential to limit growth in other ways. Together, these main results demonstrate the importance of considering feedbacks when proposing interventions to improve livelihoods.

This paper contributes to the literatures on poverty-disease traps and poverty traps more broadly. First, we provide a micro-foundation for a poverty-disease trap by connecting a model of schistosomiasis infection to a micro model of a household maximizing utility subject to their budget and production constraints. The current literature on poverty-disease traps focuses on communities and countries by creating an explicit link between income and infection (Bonds et al., 2010; Ngonghala et al., 2014, 2017). By rooting the poverty-disease trap in a microeconomic model of household decision-making, we further expand the idea of a poverty-disease trap to something that can affect an individual household or their broader community. Second, in building a micro foundation for a poverty-disease trap, we expand upon the existing micro-level poverty trap literature, which largely ignores infectious disease mechanisms (Barrett, Carter & Chavas, 2019). Household-level poverty traps typically are conceptualized as asset-based (Barrett et al., 2006; Lybbert et al., 2004; Lybbert, Just & Barrett, 2013; Toth, 2015; Zimmerman & Carter, 2003). The more recent literature expanded the causes of household-level poverty traps to include underdeveloped financial markets, loss of soil productivity and poor nutrition (Barrett & Bevis, 2015; Barrett & Swallow, 2006; Barrett & Carter, 2013; Kraay & McKenzie, 2014; Lybbert et al., 2004). There also is a long-standing literature on nutrient poverty traps built on the idea of efficiency wages whereby some subsets of workers are low capacity and are involuntary unemployed as their productivity is below the wage rate (Bliss & Stern, 1978; Dasgupta, 1993; 1997; Dasgupta & Ray, 1986, 1987; Ray & Streufert, 1993; Stiglitz, 1976). Unable to buy enough food, these individuals become trapped in poverty. Our model relates closely to this literature on nutritional-based

poverty traps as we link health status with labor productivity. By developing a model where household incomes and productivity decreases as infection restricts their labor, we add infectious disease as another cause of a household-level poverty trap.

The rest of the paper is organized as follows: section 2 provides a brief literature review of poverty-disease traps and discusses the context of the study. We introduce the model in section 3 and present the main simulation results in section 4. Section 5 discusses and concludes.

CHAPTER 2

LITERATURE AND CONTEXT

2.1 Poverty-Disease Traps

Poverty-disease traps, perhaps first proposed by Bonds et al. (2010), connect a classic susceptible-infected-susceptible (SIS) general disease model to income where key model parameters that define death, recovery, transmission, and general infection are functions of income, and income is a function of infection. Expansions of this model include Berthélemy et al. (2013), Garchitorena et al. (2015), Goenka and Liu (2020), Ngonghala et al. (2014, 2017), Pluciński, Ngonghala and Bonds (2011), and Pluciński et al. (2013). These models fall into two broad categories, those that maintain the basic feedback loop of Bonds et al. (2010) but add stochasticity or other refinements (Pluciński, Ngonghala & Bonds, 2011) and those that apply the idea of a poverty-disease trap to other modeling frameworks (Berthélemy et al., 2013; Goenka & Liu, 2020; Ngonghala et al., 2014, 2017; Pluciński et al., 2013).

The primary extension of the basic model in the literature comes from connecting a neoclassical growth model to a disease ecology model where capital accumulation depends on infection (Ngonghala et al., 2014; Pluciński et al., 2013). Both Pluciński et al. (2013) and Ngonghala et al. (2014) find evidence of poverty traps in these systems, but both models lack a micro-economic foundation whereby individuals make decisions. Ngonghala et al. (2017) develops 11 different versions of the basic neoclassical growth model that include up to three types of capital (human, physical, and biological) and populations of natural enemies, parasites, pests, and predators. Goenka and Liu (2020) add public or private investment to control disease

transmission to the macro-level neoclassical growth model. The authors find disease slows growth and makes poverty traps possible. These neoclassical growth models consider only larger aggregates of people: villages or countries.

Berthélemy et al. (2013) and Garchitorena et al. (2015) also look at individual or household decision making relating to malaria in Uganda (Berthélemy et al., 2013) and Buruli ulcer (Garchitorena et al., 2015). Berthélemy et al. (2013) use theoretical models to derive the infectiousness of malaria and then demonstrate under which conditions the spread of malaria results in a poverty trap. Garchitorena et al. (2015) model the individual or household with a Cobb-Douglas production function and they find that even with relatively low incidence of disease, as with Buruli ulcer, poverty-disease traps are possible, especially when areas start with high levels of poverty. However, the economic model does not include clear modelling of decision making at the margin, instead the authors model the decision to treat a disease with random draws based on probability distributions.

In this paper, the base of the model is the household, which makes optimal decisions and faces trade-offs due to binding budget and time constraints. By explicitly stating the optimization problem of the household with the constraints they face, we demonstrate that households can be trapped in poverty due to infectious disease. Additionally, we consider comparative statics, where we explore how changes in prices or quantities of goods impact the household's optimal decisions in addition to empirically simulating the system to allow us to better identify feedback loops within the system.

2.2 Senegalese Context

The geographical context for this paper is the Senegal River Valley and the Saint Louis and Louga regions in northern Senegal. The 1988 construction of the Diama dam, near the mouth of the Senegal River, dramatically changed land use in the region, particularly along the shores of the Senegal River and Lac de Gueirs, the largest basin within the region (Varis, Stucki, & Fraboulet-Jussia, 2006; Léger et al., 2020). The creation of irrigation canals and the subsequent desalination of the water expanded the habitat of *Bulinus* and *Biomphalaria* snails, the intermediate vector for schistosomiasis transmission. *S. mansoni* and *S. haematobium* are currently endemic within the region (Léger et al., 2020). About 75% of school children within 16 villages in the region were infected with *S. haematobium*, a urinary tract schistosomiasis infection, while 25% of school children were infected with *S. mansoni*, a colorectal infection. Many of the children infected with *S. mansoni* were also infected with *S. haematobium* (Rohr et al., 2022). Around 90% of cattle within the region were infected with *Schistosomiasis bovis* (a livestock variant of schistosomiasis), and that many of the *S. haematobium* infections within humans in the region are *S. haematobium* - *S. bovis* hybrid infections (Léger et al., 2020).

Villages within the region are small, with populations between 1,000 and 5,000 residents (Rohr et al., 2022). Households within this region are largely agricultural, predominately growing rice, millet, cowpea, and peanuts (WAEMU Commission, 2018-2019). Other horticulture crops are commonly grown in smaller plots. Many households within these villages rely on surface water sources to wash clothes, bathe, and irrigate plots. There also is sugar cane production along the northern edge of Lac

de Gueirs which contributes to significant fertilizer runoff and ecological concerns, particularly eutrophication, within the lake. Rohr et al. (2019), Hoover, Rumschlag, et al. (2020), and Lund et al. (2021) show that increased nutrient loading within the water source contribute to the growth *Ceratophyllum*, the aquatic vegetation that is the preferred habitat for snails, and thereby to increased schistosomiasis infection.

The 2018-2019 Harmonized Survey on Household Living Standards in Senegal collected by the WAEMU Commission (2018-19)¹ reports that 30% of the household heads in the survey are female, and on average household size is large with over 10 members per household (Table 2.1). The average household head is 52 years old and over 85% of household heads are married. Literacy rates are low as just under a third of household heads can read and write in French. Just under 30% of households engage in rice cultivation, around 40% of households have irrigation on at least one of their plots, and 45% of households use fertilizer on at least one of their plots. Households devote just under 400 person days to working on their farm across all family members. Just over 40% of households hire outside labor to work on their farm and the average family hires outside labor for 23 person days. Conditional on households hiring any outside labor, households hire on average outside labor for almost 35 person days.

¹ Source: WAEMU Commission, Harmonized Survey on Household Living Standards, Senegal 2018-2019. Ref. SEN_2018_EHCVM_v02_M. Dataset downloaded from www.microdata.worldbank.org on September 2, 2022.

Table 2.1: Summary Statistics of Agricultural Households in the Saint Louis and Louga Regions

	N	Mean	St. Dev.	Min	Max
<i>Household Head</i>					
Female (1 = yes)	984	0.287	0.452	0	1
Age (years)	984	52.725	14.269	20	95
Married (1 = yes)	984	0.854	0.354	0	1
Read French (1 = yes)	983	0.312	0.464	0	1
Write French (1 = yes)	983	0.306	0.461	0	1
Formal School (1 = yes)	983	0.304	0.460	0	1
<i>Household</i>					
Household Size (persons)	984	10.643	6.675	1	58
Household Farm Labor (person days)	384	388.672	462.713	0	2909
Hire Outside Labor (1 = yes)	384	0.430	0.496	0	1
Outside Labor (person days)	394	23.388	55.696	0	348
Rice (1 = yes)	384	0.273	0.446	0	1
Millet (1 = yes)	384	0.242	0.429	0	1
Cowpea (1 = yes)	384	0.474	0.500	0	1
Peanut (1 = yes)	384	0.466	0.500	0	1
Irrigation (1 = yes)	384	0.378	0.485	0	1
Fertilizer (1 = yes)	378	0.457	0.499	0	1

Notes: Summary statistics for households in the Saint Louis and Louga regions of the 2018-2019 Harmonized Survey on Household Living Standards in Senegal.

Household size is calculated by summing the number of household members included in the member module of the survey. Household farm labor and outside labor includes labor of all household members across the following tasks: preparing the plot, weeding, and harvesting. Female indicates that the household head is female. Read French and Write French indicate that the household head can read or write in French, respectively. Formal school indicates that the household head attended formal schooling. Hire outside labor indicates that the household hired at least one person day of labor from an individual outside the family. Rice, Millet, Cowpea, and Peanut indicates that the household is engaged in rice, millet, cowpea, or peanut cultivation, respectively. Irrigation and Fertilizer indicate that at least one household plot is irrigated or uses fertilizer, respectively.

2.3 Aquatic Vegetation Removal

Transmission of schistosomiasis occurs through the intermediate vector of aquatic snails. The parasite enters the water source when an infected human or cow urinates or defecates in the water releasing schistosome eggs. Once in the water, the eggs release miracidia, the first parasitic larval stage that infects the aquatic snails.

After four to six weeks in an infected snail, cercariae, another larval stage of the

parasite, exit the snail. Humans become infected with schistosomiasis through water contact with cercariae that enter the body through cuts, lesions, or any other openings (Gryseels et al., 2006).

The aquatic vegetation removal intervention modeled in this paper specifically looks to disrupt the infection cycle through reduced snail habitat. *Bulinus* and *Biomphalaria* snails live in emergent vegetation, *Ceratophyllum demersum*, in the lakes and rivers of the region. This aquatic vegetation has a symbiotic relationship with the snail population and cercariae (Haggerty et al., 2020). By removing the aquatic vegetation, the snails lose their habitat and source of food and thus release fewer cercariae.

Previous experimental work in this region suggests that removing aquatic vegetation from freshwater sources can significantly reduce *S. mansoni* infection in children through decreased snail populations (Rohr et al., 2022). As such, this model focuses on *S. mansoni* gastrointestinal infection. Additionally, recent crop trials suggest that compost made from harvested vegetation increases onion and pepper yields offering a good substitute for fertilizer (Rohr et al., 2022). By producing compost from aquatic vegetation sourced from the system, nitrogen applied on the fields in the form of compost from this vegetation simply recycles nitrogen that already existed within the system. Vegetation removal thus has the possibility to close nitrogen loops within the region. Additional details about the intervention can be found in Rohr et al. (2022).

CHAPTER 3

BIOECONOMIC MODEL

The bioeconomic model has two submodels. The first describes the disease ecology mapping how the schistosome, aquatic vegetation, and snail populations co-evolve, and relates these populations to human infections. The second, an agricultural household submodel, describes how utility maximizing households make decisions about where to allocate their labor. We begin by describing the household's problem before turning to the disease ecology submodel and finally discussing the connections between the two.

3.1 The Household's Problem

The household's problem is a variant of the non-separable agricultural household model in which consumption and production decisions become inextricably linked by multiple market failures that typically characterize poor rural villages like those in our setting (Singh, Squire, & Strauss, 1986). The economic model begins with the household, which maximizes utility, defined over consumption of food, consumption of an aggregate household good², leisure, and the health status of members of the household. We assume that utility is well-defined, increasing in all its arguments, and concave. We model the household's nutrient intake via food consumption. The health production function is Cobb-Douglas in food consumption and the fraction of household members infected scales the health status down as the fraction infected increases. Health status increases with food consumption, representing the value of more nutrition. The household can only influence their health

² The aggregate household good represents all non-food goods and services a household can consume that are available on the market.

status through more food consumption or a lower infection prevalence as there is no market for health status.

The household engages in agricultural production. The main decisions facing the household are how to allocate time and money. They can choose to allocate time between cultivating food, harvesting aquatic vegetation, or leisure. We develop a general model including the possibility of a labor market to fully capture all relevant household decisions. However, to fit the Senegalese context where most individuals work on their own farms, we abstract away from the labor market in the simulations to focus on the trade-off between working on their own farm, harvesting aquatic vegetation, and leisure. Because aquatic vegetation is a common pool resource, there is no market for aquatic vegetation, either in the water or as harvested vegetation. Thus, the multiple market failures in health status and aquatic vegetation together create non-separability between the household's production and consumption decisions. We also assume that there is no land market. Harvested vegetation becomes compost, which increases agricultural productivity (Rohr et al., 2022). Households produce food using land, labor, fertilizer, and compost from harvested aquatic vegetation. Consistent with experimental evidence from Rohr et al. (2022), compost and urea fertilizer are substitutes.³ Harvesting vegetation only requires labor.⁴ The household's production of food is a constant elasticity of substitution (CES)

³ Since both urea and compost mainly contribute nitrogen to the production process, this makes sense as adding more nitrogen from fertilizer when the crops already get nitrogen from compost should not increase productivity at the same rate as the initial compost or fertilizer treatment.

⁴ While it requires a pit to convert vegetation into compost, we assume that there exists sufficient unused and free land within the village such that land is not a constraint to the production of compost.

production function while harvesting vegetation uses Cobb-Douglas production technology.⁵

Let i denote the different goods a household consumes, produces, or uses as an input to production. Let q_i denote the quantity of goods produced or used as inputs in the production process by the household. The household produces ($q_i \geq 0$) of food ($i = f$) using land ($i = d$), labor ($i = l_f$), fertilizer ($i = u$), and compost (ωq_v). The household makes compost from harvested vegetation ($i = v$) and harvesting vegetation requires labor ($i = l_v$). Composting reduces the mass of harvested vegetation, so the fraction of harvested vegetation remaining as compost to use in food production is $\omega \in (0,1)$. Households can also hire labor to produce food L_f^h or harvest vegetation L_v^h . Let $L_f = q_{l_f} + L_f^h$ be the total amount of labor used in the production of food and $L_v = q_{l_v} + L_v^h$ be the total amount of labor used to harvest vegetation. The household's production technology for food is then given by $F(L_f, q_d, q_u, \omega q_v)$ and the production technology for harvesting vegetation is $G(L_v)$.

Let \mathbf{c} denote the vector of all consumption goods comprised of food ($i = f$), non-food household goods and services ($i = g$), and leisure ($i = l$). Let $H(I_1, S_1, c_f)$ denote the household's health status, where I_1 is the number of infected individuals in the household, S_1 is the number of not infected (susceptible) individuals in the household,⁶ and c_f is food consumption. We denote household utility as $U(\mathbf{c}, H)$.

⁵ Since labor is the only input to harvest vegetation, allowing for substitution between inputs as in a CES production function is unnecessary.

⁶ We follow the notation of Gao et al. (2011) for infected (I_1) and susceptible individuals (S_1). We will use similar notation for infected and susceptible snails (I_2 and S_2). We use the subscript 1 for humans and the subscript 2 for snails.

Each household has endowments of labor e_l and land e_d in each time period. Each household member has one unit of labor; however, infection reduces the labor availability of an individual to τ where $0 \leq \tau < 1$. Infection reduces nutrient absorption from food and overall results in less labor productivity, effectively reducing the labor availability of infected individuals. The labor available to the household a_l is the sum of the labor availability of all individual household members. A household generates income by growing food and selling its labor in the local labor market, L^m . The household hires and sells labor at wage w . There are perfectly competitive markets for food, the aggregate household good, labor, and urea fertilizer (the tradables set $T = \{f, g, l, u\}$), but there are not markets for vegetation, land or health (the non-tradables set $NT = \{d, v, H\}$). Each household must fully self-provide non-tradable goods. Finally, let p_i denote the market price for good i .

Thus, in each period, the household solves the problem:

$$\max_{(c,q)} U(c, H) \quad (1)$$

subject to the cash budget constraint for tradable goods,

$$p_f c_f + p_g c_g \leq p_f \left(F(L_f, q_d, q_u, \omega q_v) \right) - p_u q_u - w(L_f^h + L_v^h) + wL^m \quad (2)$$

the availability constraint for vegetation use,

$$q_v - \beta_v (L_v)^{\gamma_1} \geq 0 \quad (3)$$

the availability constraint for land use,

$$q_d - e_d \geq 0 \quad (4)$$

the time constraint on the household's labor availability,

$$a_l \geq q_{l_f} + q_{l_v} + L^m + c_l \quad (5)$$

and the health production function.

$$H = H(I_1, S_1, c_f) \quad (6)$$

We substitute the availability constraint into the food production function in the cash budget constraint and then substitute the labor constraint into the budget constraint to create the full income constraint:

$$p_f c_f + p_g c_g + w (c_l + q_{l_f} + q_{l_v}) \leq p_f \left(F \left(q_{l_f}, L_f^h, q_d, q_u, \omega q_v(q_{l_v}, L_v^h) \right) \right) - p_u q_u - w (L_f^h + L_v^h) + w a_l \quad (7)$$

Requiring all land to be used in production, assuming an interior solution, substituting (6) into (1) and using Lagrange multiplier λ on the household's full income constraint, the first order conditions for the maximization problem are:

$$\frac{\partial U}{\partial c_f} + \frac{\partial U}{\partial H} \frac{\partial H}{\partial c_f} = \lambda p_f \quad (8)$$

$$\frac{\partial U}{\partial c_g} = \lambda p_g \quad (9)$$

$$\frac{\partial U}{\partial c_l} = \lambda w \quad (10)$$

$$p_f \frac{\partial F}{\partial q_{l_f}} = w \quad (11)$$

$$p_f \frac{\partial F}{\partial q_v} \frac{\partial q_v}{\partial q_{l_v}} = w \quad (12)$$

$$p_f \frac{\partial F}{\partial L_f^h} = w \quad (13)$$

$$p_f \frac{\partial F}{\partial q_v} \frac{\partial q_v}{\partial L_v^h} = w \quad (14)$$

$$p_f \frac{\partial F}{\partial q_u} = p_u \quad (15)$$

Equations (8), (9), and (10) can be rearranged to show that the ratio of the marginal benefit of consuming food (which includes direct increases in utility and indirect utility increases through improved health) to the marginal benefit of consuming the aggregate household good or leisure equals the price ratio. Equations (11) – (15) are input use constraints that require that family labor, hired labor, and fertilizer is used until the value of the marginal product of labor or fertilizer equals its respective cost or opportunity cost in the case of family labor.

Specifically, assume that the household has Cobb-Douglas utility:

$$U(\mathbf{c}, H) = c_f^{\theta_f} c_g^{\theta_g} H^{\theta_h} c_l^{\theta_l} \quad (16)$$

where the θ 's add up to one. We calibrate the parameters $\boldsymbol{\theta}$ by estimating expenditure shares from the Harmonized Survey on Household Living Standards 2018-2019 in Senegal (WAEMU Commission, 2018-2019). Expenditure shares can be found in Table 3.1. We set $\theta_f = 0.55$, $\theta_g = 0.3$, $\theta_h = 0.1$, and $\theta_l = 0.05$.

Table 3.1: Estimated Expenditure Shares

	N	Mean	St. Dev.	Min	Max
Food Expenditure Share	7156	0.539	0.131	0.027	0.941
Household Good Expenditure Share	7156	0.313	0.126	0.007	0.971
Health Expenditure Share	6035	0.036	0.052	0	0.798

Notes: Estimated expenditure shares from the Harmonized Survey on Household Living Standards in Senegal collected in 2018 and 2019. We classified goods according to three categories: food, health, and household goods where household goods captured goods that did not clearly fit into food or health. We then aggregated annual expenditure for each of the goods in these categories. Some expenditures recorded in the survey were excluded, therefore the totals may not add up to 1.⁷ Fewer households report cash health expenditures, so we take these expenditure share estimates as a lower bound when calibrating the household's utility function focusing on the expenditure share estimates for food and household goods.

Health status follows the health production function given by

$$H = \exp\left(\frac{S_1}{I_1 + S_1}\right) c_f^{h_f} \quad (17)$$

where I_1 is infected household members, S_1 is not infected household members, and h_f is the elasticity of the increase in health from food consumption and we set $h_f = 0.000384$ (Foster & Rosenzweig, 1994; Pitt, Rosenzweig & Hassan, 1990).

Production of food takes the CES form:

$$q_f = \left(\alpha_d q_d^\phi + \alpha_l (q_{l_f} + L_f^h)^\phi + \alpha_u q_u^\phi + \alpha_v (\omega q_v)^\phi \right)^{1/\phi} \quad (18)$$

We estimate factor cost shares from the Harmonized Survey on Household Living Standards 2018-2019 in Senegal to determine the parameters α_d , α_l , α_u , and α_v and calibrate ϕ to achieve fertilizer use consistent with observed patterns (WAEMU Commission, 2018-2019). Estimated factor cost shares can be found in

⁷ We exclude alcohol and tobacco purchases. Since we abstract away from the land market, we exclude any payments for land or housing.

Table 3.2. We set $\alpha_d = 0.26$, $\alpha_l = 0.64$, $\alpha_u = 0.05$, $\alpha_v = 0.05$, and $\phi = 0.4$. We consider labor shares in the model, but scale the production function to labor days based on the average amount of labor allocated to a plot within the survey data to scale labor inputs in the production of food as the unit of labor is important for understanding the returns to labor (McCullough, 2017)

Table 3.2: Estimated Factor Cost Shares

	N	Mean	St. Dev.	Min	Max
Land Factor Cost Share	2892	0.281	0.221	0	1
Labor Factor Cost Share	2892	0.658	0.249	0	1
Inorganic Fertilizer Factor Cost Share	2892	0.048	0.109	0	0.996
Compost Factor Cost Share	1277	0.052	0.095	0	1

Notes: Estimated factor cost shares from the Harmonized Survey on Household Living Standards in Senegal collected in 2018 and 2019. We measure land in hectares and then valued land using the median land rental price in the Senegalese Agricultural Household Survey (DAPSA, 2017-2018). We then calculated a household's total labor days on each plot by the following tasks: prepping the land, weeding, and harvesting. We include both family and hired labor and then calculate total labor by adding up all of the labor days on each of the family's plots including all three tasks. We then use the median adult male harvesting wage in each region as the value of each day of labor to calculate the total cost of labor. Inorganic fertilizer includes urea, NPK, and phosphates and is measured in kgs. We use the median regional price for each type of inorganic fertilizer when calculating the factor cost. Compost is also measured in kgs. As with inorganic fertilizer, we use the median regional price for animal compost to calculate the factor cost. All carts and sacs are assumed to be 50 kg of fertilizer or animal compost.

We model vegetation harvest as

$$q_v = \beta_v (q_{l_v} + L_v^h)^{\gamma_1} \quad (19)$$

where we set $\beta_v = 14.4942$ and $\gamma_1 = 0.2595$ using estimates of harvested vegetation and labor data from Rohr et al. (2022).⁸ We set the price of food, $p_f = 290$ FCFA to

⁸ Details of the estimation can be found in Appendix A and regression results are in Table 8.

the average, location adjusted price of local rice estimated from Senegalese price reports (ANSD, 2018-2019). We estimate the price of urea from the 2017 agricultural household survey performed by the Direction de l'Analyse, de la Prévision et des Statistiques Agricoles de la République du Sénégal (DAPSA) and set $p_u = 270$ FCFA (DAPSA, 2017-2018). We set the price of the aggregate household good to $p_g = 500$ FCFA. Finally, we eliminate the local labor market from the baseline simulations to model decision making when households spend most of their time producing food on their own farm to match the setting. In the simulations, we normalize all prices setting the price of food equal to one. A summary of the parameter values used in the household model is presented in Table 3.3.

Table 3.3: Parameters for the Household Model

Parameter	Description	Value
θ_f	Utility function coefficient on food	0.55
θ_g	Utility function coefficient on household goods	0.3
θ_h	Utility function coefficient on health status	0.1
θ_l	Utility function coefficient on leisure	0.05
h_f	Coefficient on food consumption in health status function	0.000384
α_d	Coefficient on land in food production	0.26
α_l	Coefficient on labor in food production	0.64
α_u	Coefficient on fertilizer in food production	0.05
α_v	Coefficient on vegetation in food production	0.05
ω	Vegetation retained in composting	0.6
ϕ	Substitution parameter	0.4
β_v	Coefficient for harvesting vegetation	14.4942
γ_1	Exponent on labor in harvesting vegetation	0.2595
p_f	Price of food	290 FCFA
p_h	Price of household good	500 FCFA
p_u	Price of fertilizer	270 FCFA

Notes: The θ parameters for the utility function are based off of household expenditure share estimates from the Saint Louis and Louga regions in the Harmonized Survey on Household Living Standards reported in Table 3.1. We round the expenditure share estimates for food and household goods and then scale the parameters on health status and leisure so that the sum of all θ 's add up to one. The parameter h_f is taken from Pitt, Rosenzweig and Hassan (1990)'s estimate of the relationship between caloric intake and health. We scale the estimate to fit our measure of calories in one kg of rice which is the unit of food in the model. The α parameters for the food production function are based off of factor cost share estimates from the Saint Louis and Louga regions in the Harmonized Survey on Household Living Standards reported in Table 3.2. We round the factor cost share estimates so that the α 's add up to one. The substitution parameter ϕ is calibrated to achieve fertilizer use levels consistent with the Senegalese context. The mass loss during compost, modeled by the parameter ω , is based on the range of estimates in Şevik, Tosun and Ekinci (2018) and calibrated to achieve fertilizer use consistent with the Senegalese context. The parameters β_v and γ_1 are estimated from data on vegetation removal done in Rohr et al. (2022) and reported in Appendix A. The price of food comes from Senegalese price reports released by ANSD and the price of fertilizer is taken from the Senegalese agricultural household survey in 2017 conducted by DAPSA. The price of the household good is calibrated to capture the value of many possible consumption goods the household purchases which are more expensive than food.

For comparison with the recent state of the system before informing people of the prospective value of using harvested aquatic vegetation as compost, we also present a simplified version of the model without aquatic vegetation harvest. In this case, households can no longer use labor to harvest vegetation or produce any compost. This simulation represents the current status quo. Our core comparisons thus simulate the equilibrium effects of making villagers aware of the prospective value of composting harvested aquatic vegetation.

3.2 Disease Ecology Model for Schistosomiasis

The disease ecology model tracks the populations of aquatic vegetation (*Ceratophyllum*, N), miracidia (larval schistosomes that infect snails, M), infected and susceptible snails (I_2 and S_2), cercariae (larval schistosomes that infect humans, P), and infected and susceptible humans (I_1 and S_1). We adapt the model of schistosomiasis disease ecology in Gao et al. (2011) to fit the Senegalese context and down-scale the parameters from a large community to one that matches the household-level simulations. More details about the adjustments are provided in Appendix B. Relative to the human lifespan, the cycle of schistosomiasis infection is relatively short. Cercariae live around 10 hours, miracidia live around 25 hours, and snail infections last around 100 days (Liberatos, 1987). Therefore, very few or none of the existing cercariae or miracidia population will survive over the course of the year creating challenges for matching the timescale across the household and disease ecology submodels. Converting the continuous time disease ecology submodel to discrete time to match the household submodel requires significant linearization and assumptions about annual changes in miracidia, cercariae, and snail populations that

can cause meaningful aggregation errors. To avoid magnifying aggregation errors, we use a continuous time disease ecology submodel that better matches the timeline of the schistosomiasis infection cycle. We simulate annual changes by simulating the system of differential equations forward 365 days, where all parameters are given in daily rates.

The *Ceratophyllum*, the keystone species of aquatic vegetation, population follows a logistic growth function. The population also depends on the amount of vegetation removed by household members or hired workers q_v . With a starting density of N_0 , the population density of aquatic vegetation is

$$\frac{dN}{dt} = r \times N \times \left(1 - \frac{N}{K}\right) \quad (20)$$

where r is the net growth rate of *Ceratophyllum*, and K is the carrying capacity of the freshwater environment. The amount of aquatic vegetation to start each period is

$N_{t+1} = N_t - q_{v_t} + \rho \times q_{u_t} \times N_t$ where q_{v_t} is the amount of harvested aquatic vegetation, i.e., the household's production of harvested vegetation and $\rho \times q_{u_t} \times N_t$ captures the impact of urea fertilizer use, q_{u_t} , on vegetation growth as Rohr et al.

(2019, 2022) reports that agrochemicals like fertilizer contribute to vegetation growth.

We estimate the carrying capacity and starting value of *Ceratophyllum* based on the average amount of vegetation found within water access points sampled by Rohr et al. (2022), setting $K = 9.007kg$ and $N_0 = 9.007kg$. We set $r = 0.05$ and $\rho = 0.1$. Table 3.4 summarizes all parameters in the disease ecology model.

Aquatic vegetation affects the snail population, both susceptible and infected, which we model by

$$\frac{dS_2}{dt} = \Lambda_2 - \frac{\beta_2 MS_2}{M_0 + \epsilon M^2} - (\mu_2 + \chi(K - N))S_2 \quad (21)$$

$$\frac{dI_2}{dt} = \frac{\beta_2 MS_2}{M_0 + \epsilon M^2} - (\mu_2 + \delta_2 + \chi(K - N))I_2 \quad (22)$$

where Λ_2 is the recruitment rate of susceptible snails, β_2 is the probability of snail infection from miracidia, M_0 is the contact rate between miracidia and snails, ϵ is the saturation coefficient for miracidial infectivity, μ_2 is the natural death rate of snails, δ_2 is the death rate of snails from infection, and χ is the death rate of snails from a one kg decrease in vegetation. We set $M_0 = 1.0 \times 10^6$, $\epsilon = 0.3$, $\Lambda_2 = 100$, $\beta_2 = 0.615$, $\mu_2 = 0.008$, and $\delta_2 = 0.0004012$ (Gao et al., 2011) while we estimate $\chi = 0.02842$ from aquatic vegetation removal data (Rohr et al., 2022).⁹

The miracidia population follows

$$\frac{dM}{dt} = k\lambda_1 I_1 - \mu_3 M \quad (23)$$

where k is the number of eggs released into the environment per human host, λ_1 is the hatching rate for miracidia, and μ_3 is the miracidial mortality rate. We set $k = 300$, $\lambda_1 = 50$, and $\mu_3 = 2.5$ (Gao et al., 2011; Nguyen et al., 2021). The cercariae population follows

$$\frac{dP}{dt} = \lambda_2 I_2 - \mu_4 P \quad (24)$$

where λ_2 is the cercarial emergence rate and μ_4 is the cercarial mortality rate. We assume there is no cercarial elimination intervention. We estimate the model with $\lambda_2 = 2.6$ and $\mu_4 = 0.004$ (Gao et al., 2011).

⁹ We estimate χ using a simple calculation comparing the average mass of aquatic vegetation removed at each site to the average drop in snail population after removal.

Finally, the susceptible and infected human populations follow

$$\frac{dS_1}{dt} = -\frac{\beta_1 P S_1}{1 + \alpha_1 P} + \eta I_1 \quad (25)$$

$$\frac{dI_1}{dt} = \frac{\beta_1 P S_1}{1 + \alpha_1 P} - \eta I_1 \quad (26)$$

Where β_1 is the contact between cercariae and humans, α_1 is the saturation coefficient for cercarial infectivity, and η is the treatment rate of infected humans. We assume that schistosomiasis infections cause neither birth nor deaths of humans. The unconditional mortality rate of humans due to schistosomiasis is around $\frac{1}{1,000}$ (Verjee, 2019). Since we consider villages with average populations around 5,000 with infections around 1,000 – 4,000 at any given time, deaths from schistosomiasis are relatively rare. Thus, we abstract away from the disease's mortality effects and instead focus on the morbidity impacts through reduced labor productivity. Because we only consider relatively short time periods, we treat the household population as stable and focus on labor availability dynamics within the household. We set $\beta_1 = 1.766 \times 10^{-8}$ and $\alpha_1 = 0.8 \times 10^{-8}$ (Gao et al., 2011). We set $\eta = 0.0068$ to model some infected individuals receiving treatment through deworming medications like praziquantel during sporadic mass deworming events. However, it is expensive to diagnose schistosomiasis and thus the treatment of infections remains relatively infrequent.

Table 3.4: Parameters for the Disease Ecology Model

Parameter	Description	Value
r	Vegetation growth rate	0.05
K	Vegetation carrying capacity	9.007 kg
ρ	Effect of fertilizer on vegetation growth	0.1
Λ_2	Snail recruitment rate	100
β_1	Contact between cercariae and humans	1.766×10^{-8}
β_2	Probability of snail infection from miracidia	0.615
μ_2	Snail natural mortality rate	0.008
μ_3	Miracidial mortality rate	2.5
μ_4	Cercarial mortality rate	0.004
δ_2	Snail death rate from infection	0.0004012
λ_1	Hatching rate of miracidia	50
λ_2	Cercarial emergence rate	2.6
α_1	Saturation coefficient for cercarial infectivity	0.8×10^{-8}
M_0	Contact rate between miracidia and snails	1.00×10^6
ϵ	Saturation coefficient for miracidial infectivity	0.30
χ	Snail death rate from vegetation removal	0.02842
k	Eggs released per infected human	300
η	Treatment rate of infected humans	0.00068

Notes: The parameters β_2 , μ_4 , λ_2 , M_0 , ϵ , and k are from Gao et al. (2011). The parameters Λ_2 , μ_2 , and δ_2 are calibrated to achieve a stable snail population throughout the simulations. The parameters λ_1 and μ_3 are calibrated to achieve a stable miracidia throughout the simulations. The parameters β_1 and α_1 are calibrated to achieve stable infection rates in humans consistent with the 25% infection rate from data collected by Rohr et al. (2022). The parameters K and χ are estimated from data collected by Rohr et al. (2022). The parameters r and ρ are calibrated to fit the high growth rate of vegetation observed in the Senegalese context and to adequately capture the effect of fertilizer runoff on vegetation growth. η is calibrated to deworming every four years.

Initial population sizes for all relevant populations in the disease ecology submodel are reported in Table 3.5.

Table 3.5: Starting Values of Disease Ecology Parameters

Parameter	Description	Value
N_0	Starting amount of vegetation	9.007 kg
S_1	Susceptible humans	7.5
I_1	Infected humans	2.5
S_2	Susceptible snails	200
I_2	Infected snails	12,300
M	Miracidia	13,000
P	Cercariae	130,000

Notes: Average household size begins at the nearest whole number with easy division into 4 of 10 based on the average household size in the Saint Louis and Louga region from the Harmonized Survey on Household Living Standards in Senegal, 2018-2019. Infected and susceptible humans were then calculated based on the average infection prevalence of *S. mansoni* in the infection data from Rohr et al. (2022). All other parameters were calibrated to be consistent with the human infection data.

3.3 Linking the Two Submodels

The disease ecology submodel and the household submodel link through the infection status of the household, which directly affects household utility and impacts the household's labor availability, and through the household's use of urea fertilizer and its vegetation harvest, which changes the vegetation population within the water source. The disease ecology submodel provides population estimates of infection, which we scale down to individual-level and household-level infection rates through stochastic realizations of infection. Infection is inherently stochastic, so we model infection using independent Bernoulli random draws for each household member at the start of each time period. The mean of the Bernoulli random draw is given by the

infection rate predicted by the disease ecology submodel, which is the population infection prevalence or $Infection\ Rate = \frac{I_1}{I_1+S_1}$. After the first period, we also take random draws for curing infection, where the mean of the Bernoulli random variable set at 0.25 which captures the fact that households in this region experience sporadic mass deworming campaigns.

Since each individual household is only one small part of a village and these villages only access a small portion of the entire aquatic system, these households do not individually influence the disease ecology submodel. Since household behavior does not individually impact disease ecology, the household does not consider the equations of the disease ecology submodel in its own optimization. In this way, the household solves a series of static, single period optimization problems as in Barrett and Arcese (1998).¹⁰ In this framework, the disease ecology submodel gives laws of motion that show how the state and the average infection rate evolve over time. In each period, we solve the household's static optimization problem and then use the household's choices to determine the amount of vegetation and the realizations of infection to determine the current infection prevalence. With these new starting populations, we simulate the disease ecology model one year forward to give the state

¹⁰ We can also assume that households don't have full control over the decisions of all of their household members, such as parents telling their children to stay of the water but children not listening or assume that households do not fully understand the evolution of the disease ecology submodel as given in the equations that connect vegetation, miracidia, cercariae, snails, and humans to eliminate the fully dynamic nature of the original problem. Any of these assumptions are likely to hold. This makes the problem computationally tractable. In a fully dynamic problem, all seven populations in the disease ecology submodel would be different state variables, which would require significant discretization or a large reduction in the number of states to solve given the curse of dimensionality in solving optimal control problems.

of infection in the next time period. The model is then solved by the following iterative process for each period in the simulation:

1. We use Bernoulli random draws to realize household infection;
2. The household solves their static problem by allocating its time and money to maximize its period-specific utility;
3. Using the realizations of infection and the household's decisions, we calculate the current aquatic vegetation population and the current number of infected and susceptible individuals. We use these starting values and simulate the disease ecology submodel forward one year and calculate the vegetation population and village infection rate in the following period;
4. Constraints on the household's choices adjust so that vegetation harvest is not above available vegetation in the next period's state;
5. Repeat from step one until we reach 20 periods.

We are interested in the within-generation results of the system to model what happens when vegetation harvest is introduced and if vegetation harvest results in a new level of equilibrium infections, so we limit the simulation time to 20 annual periods. This time frame is long enough to capture any short-term changes in the equilibrium level of schistosomiasis infection but allows us to abstract away from long-term changes, including through impaction on children's educational attainment, in human populations that would further complicate the model.

CHAPTER 4

HOUSEHOLD SIMULATIONS

We present results from simulations of three household types over a twenty-year time horizon. For each household type, we do 100 stochastic simulations to capture different optimal paths based on the realized random infection draws. Household types are determined by land holdings, which are set at the 25th percentile, 50th percentile, and 75th percentile of land holdings in the Saint Louis and Louga regions in the Harmonized Survey on Household Living Standards in Senegal 2018-2019 (WAEMU Commission, 2018-2019). Land holdings proxy for wealth in these simulations such that as land endowment increases, the wealth of the household also increases. Thus, we compare results across land holding types to determine how wealth levels impact the optimal decisions of the household. Land affects the household's optimal decision as it enters into the food production function. As the land endowment increases, the value of the marginal product of labor, vegetation, and urea will increase (equations 11, 12, and 15). Table 4.1 reports the different household types.

Table 4.1: Land Endowments for Household Simulations

Type	Land Endowment (hectares)
25 th percentile	0.5
50 th percentile	2
75 th percentile	5.5

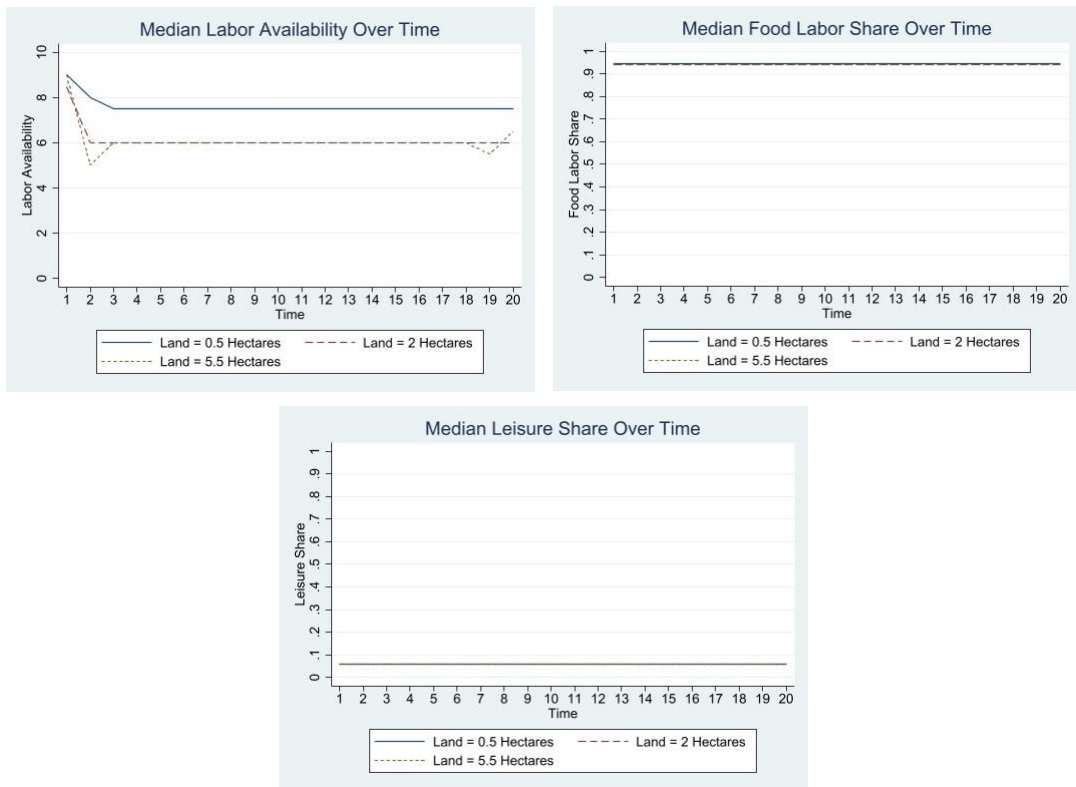
Notes: Land holdings based on the 25th, 50th, and 75th percentiles in the Saint Louis and Louga regions from the Harmonized Survey on Household Living Standards in Senegal collected in 2018 and 2019.

4.1 Simulations with No Vegetation Harvest

To begin, we start with the baseline case that represents the status quo. We eliminate the household's option to remove vegetation and produce compost by mechanically setting the marginal product of labor in aquatic vegetation harvest to zero. In this simulation, we model how households currently behave and establish a starting level of infection under current conditions. In this model, and in all main results, we also get rid of the local labor market and focus on the household engaging in agricultural production. We track the following key outcome variables: household labor availability, labor allocated to food production, leisure, fertilizer use, the vegetation load in the water source, the household's level of infection, and the household's income. We then take the median of 100 simulations for each outcome at each time period for each household land endowment. We present the results for these status quo simulations in Figures 4.1 and 4.2.

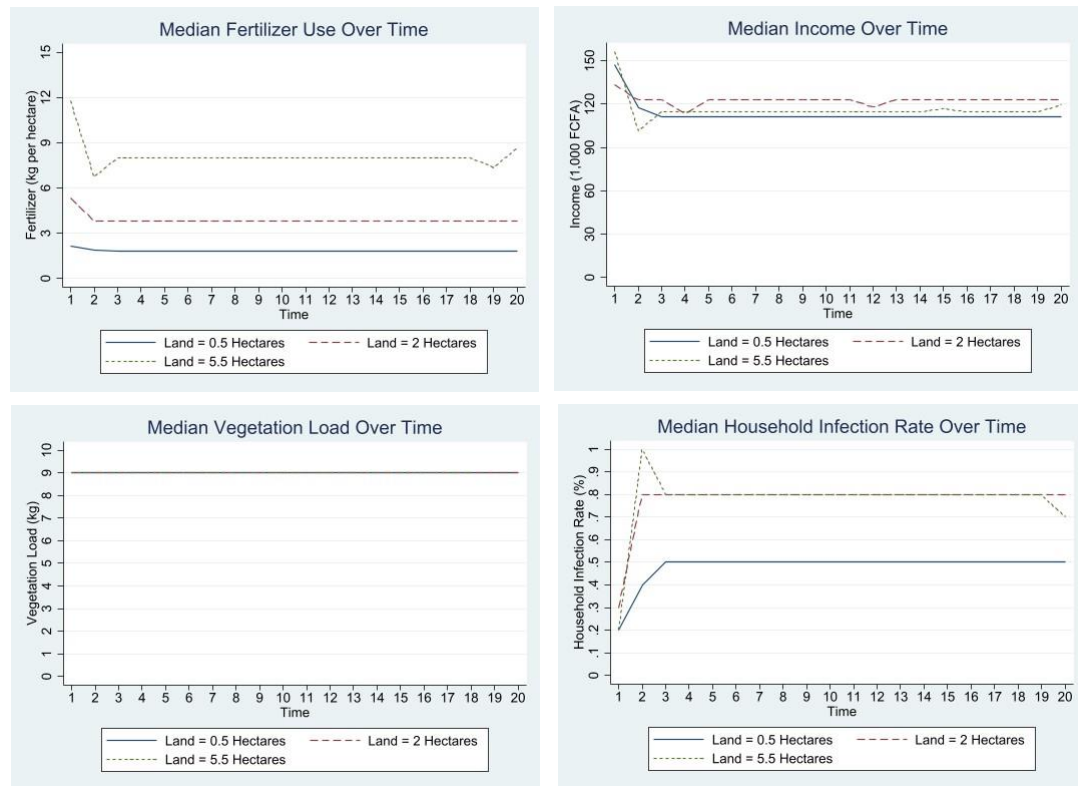
When households cannot harvest vegetation, the level of aquatic vegetation in the water source remains stable at its carrying capacity as expected (Figure 4.2). Additionally, household infection reaches a high steady state while labor availability is low (Figures 4.1 and 4.2). Households spend most of their labor on their farm and use moderate amounts of fertilizer in the production of food (Figures 4.1 and 4.2). We see that income is low as labor availability is low, resulting in a poverty trap. We find evidence of the feedback loops that create a poverty-disease trap whereby infection causes incomes to fall, which continues the cycle of both infection and poverty. These patterns are virtually identical across the wealth distribution.

Figure 4.1: Median Labor Availability and Labor Allocation Shares for Simulations without Vegetation Harvest



Notes: The top left plots the median labor availability (the labor endowment scaled based on realized infections) across 100 20-year simulations for three different household land endowments. The top right reports the median food labor share, and the bottom reports the median leisure share. Medians are within each land endowment and within each time period across the 100 simulations. Household size is 10, so the maximum labor availability is 10.

Figure 4.2: Median Fertilizer Use, Income, Household Infection Rate, and Vegetation Load for Simulations without Vegetation Harvest



Notes: The top left plots the median fertilizer use in kgs per hectare across 100 20-year simulations for three different household land endowments. The top right reports the median income in 1,000s of FCFA, the bottom left reports the median vegetation load (population) in the water source in kgs and the bottom right reports the median household infection rate. Medians are within each land endowment and within each time period across the 100 simulations. Aquatic vegetation load represents the size of the snail habitat within the village water access point used by the household. The infection rate of the household is the number of infected individuals divided by total number of household members (the number infected plus the number not infected).

4.2 Simulations with Vegetation Harvest

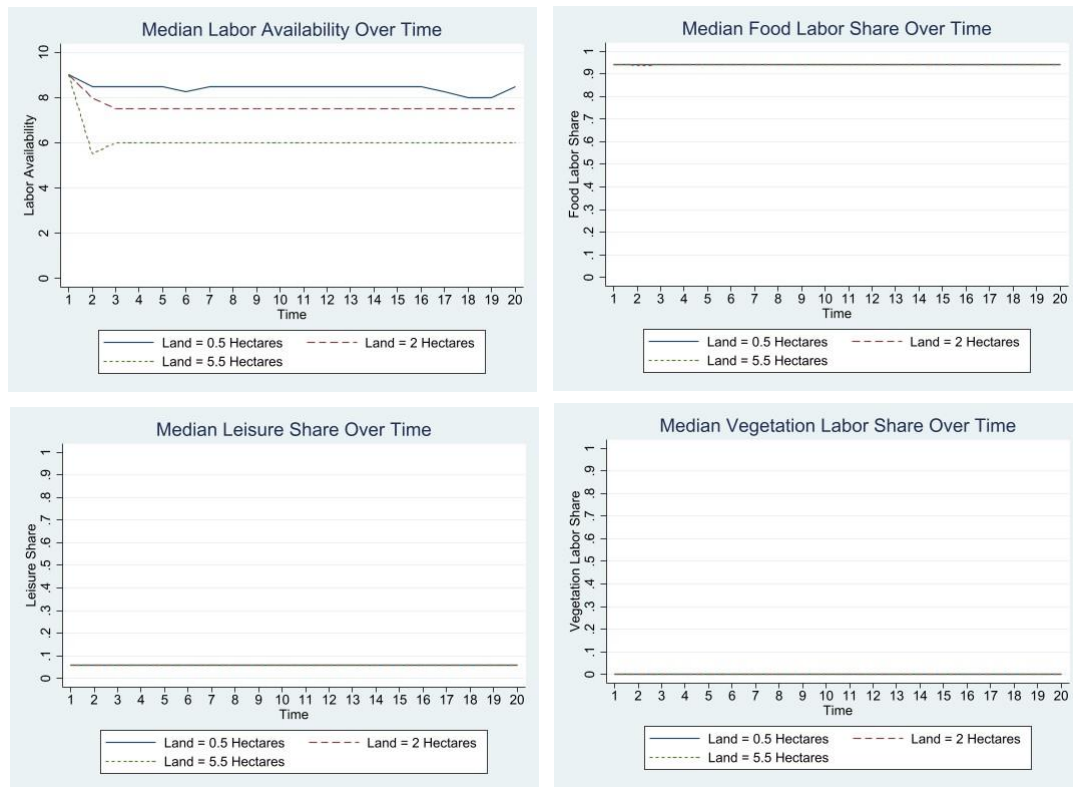
Next, we examine the case where the household can harvest aquatic vegetation.

We still abstract away from the local labor market, so in this case households can choose to provide their own labor to harvest aquatic vegetation. We limit the household's labor allocation to vegetation harvest based on the current amount of

vegetation within the water source given the vegetation population in the disease ecology submodel. We again run simulations for 20 years and do 100 simulations for each land endowment. We track the same key outcome variables. Results from the simulations with vegetation harvest are presented in Figures 4.3 and 4.4.

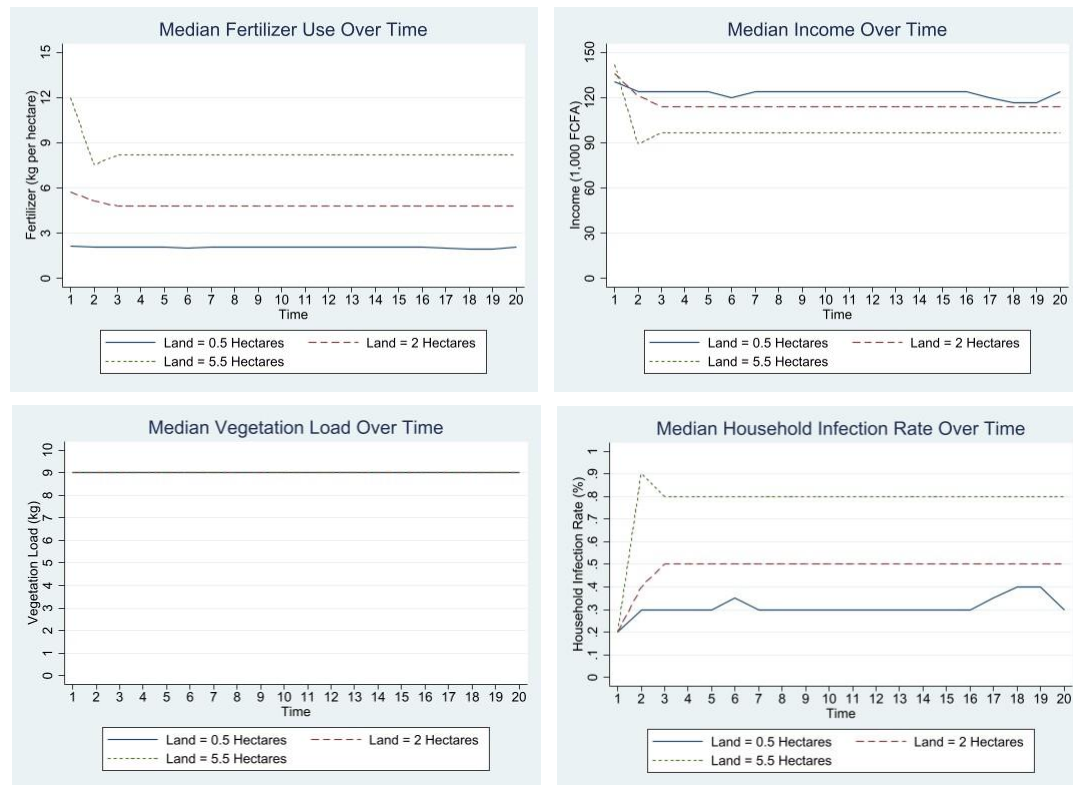
In this scenario, all household types allocate a very small fraction of their labor to vegetation harvest (Figure 4.3). Households hit the limit for vegetation harvest, but a small amount of labor is enough to temporarily clear the current vegetation from the water source, consistent with data collected in Rohr et al. (2022) where a small number of individuals (10 or less) could clear the village's water access points during a day. However, households also use fertilizer on their plots (Figure 4.4), so the vegetation load never truly reaches zero as fertilizer spurs new vegetation growth. Due to the fast growth rate of vegetation, the vegetation load fully recovers within the year, and we do not see a change in the overall year-to-year vegetation load. Relative to the case without vegetation harvest, the household infection rate settles at a lower level for both the low and middle levels of land endowment (Figure 4.4). As with the baseline case, most of the household's labor is allocated to food production (Figure 4.3). Incomes remain low in these simulations, but the median income is higher than in the baseline case without vegetation harvest (Figure 4.4). So, while simply allowing vegetation harvest with fertilizer spurring new vegetation growth cannot fully clear the water source, we do see lower levels of infection and higher incomes when vegetation harvest is introduced.

Figure 4.3: Median Labor Availability and Labor Allocation Shares for Simulations with Vegetation Harvest



Notes: The top left plots the median labor availability (the labor endowment scaled based on realized infections) across 100 20-year simulations for three different household land endowments. The top right reports the median food labor share, the bottom left reports the median leisure share and the bottom right reports the median vegetation harvest labor share. Medians are within each land endowment and within each time period across the 100 simulations. Household size is 10, so the maximum labor availability is 10.

Figure 4.4: Median Fertilizer Use, Income, Household Infection Rate, and Vegetation Load for Simulations with Vegetation Harvest



Notes: The top left plots the median fertilizer use in kgs per hectare across 100 20-year simulations for three different household land endowments. The top right reports the median income in 1,000s of FCFA, the bottom left reports the median vegetation load (population) in the water source in kgs and the bottom right reports the median household infection rate. Medians are within each land endowment and within each time period across the 100 simulations. Aquatic vegetation load represents the size of the snail habitat within the village water access point used by the household. The infection rate of the household is the number of infected individuals divided by total number of household members (the number infected plus the number not infected).

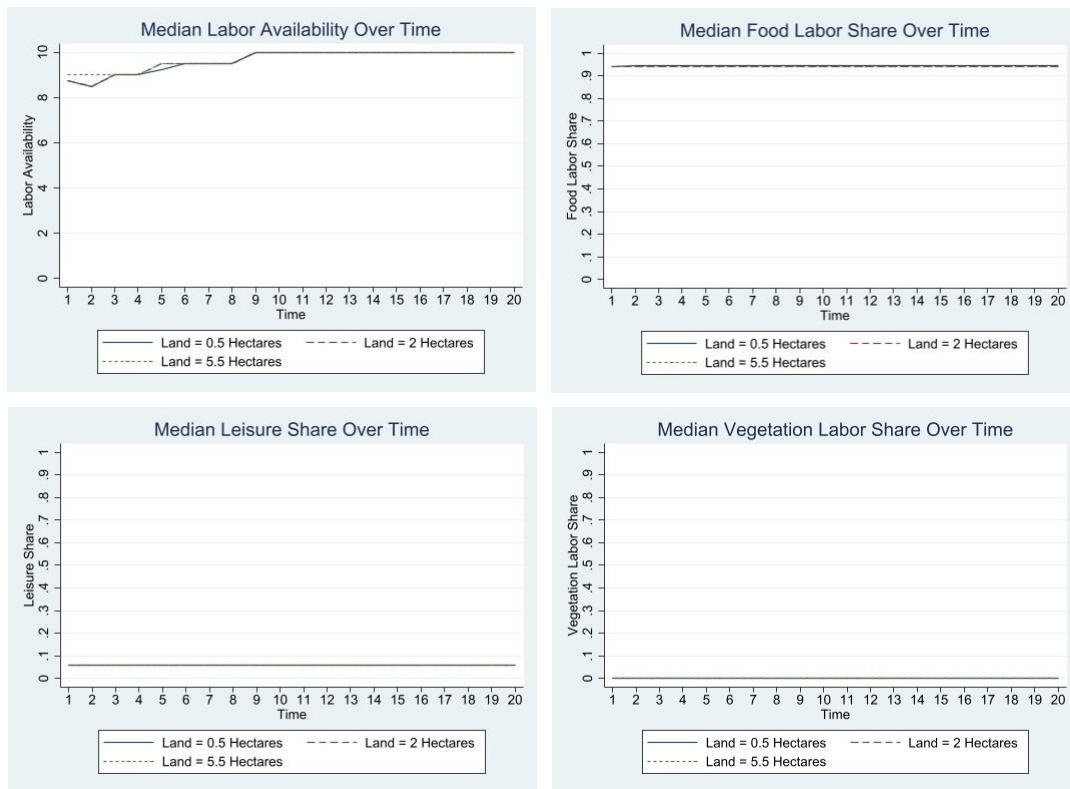
4.3 Simulations with Vegetation Harvest and No Fertilizer Effect

To further explore the impact of fertilizer spillovers, we run simulations where we eliminate the fertilizer effect on the vegetation load in the village water source. For these simulations, we set $\rho = 0$ so household fertilizer use has no impact on aquatic vegetation effectively eliminating the spillovers from fertilizer use. We hypothesize that by eliminating the small level of vegetation that is sustained throughout time by

fertilizer, households will be able to fully clear the water source of vegetation and infection levels will plummet. As with the other cases, we run simulations for 20 years and do 100 simulations for each land endowment. We track the same key outcome variables as the case with vegetation harvest and a fertilizer effect. Results of the simulations that allow for vegetation harvest and eliminate the fertilizer spillovers can be found in Figures 4.5 and 4.6.

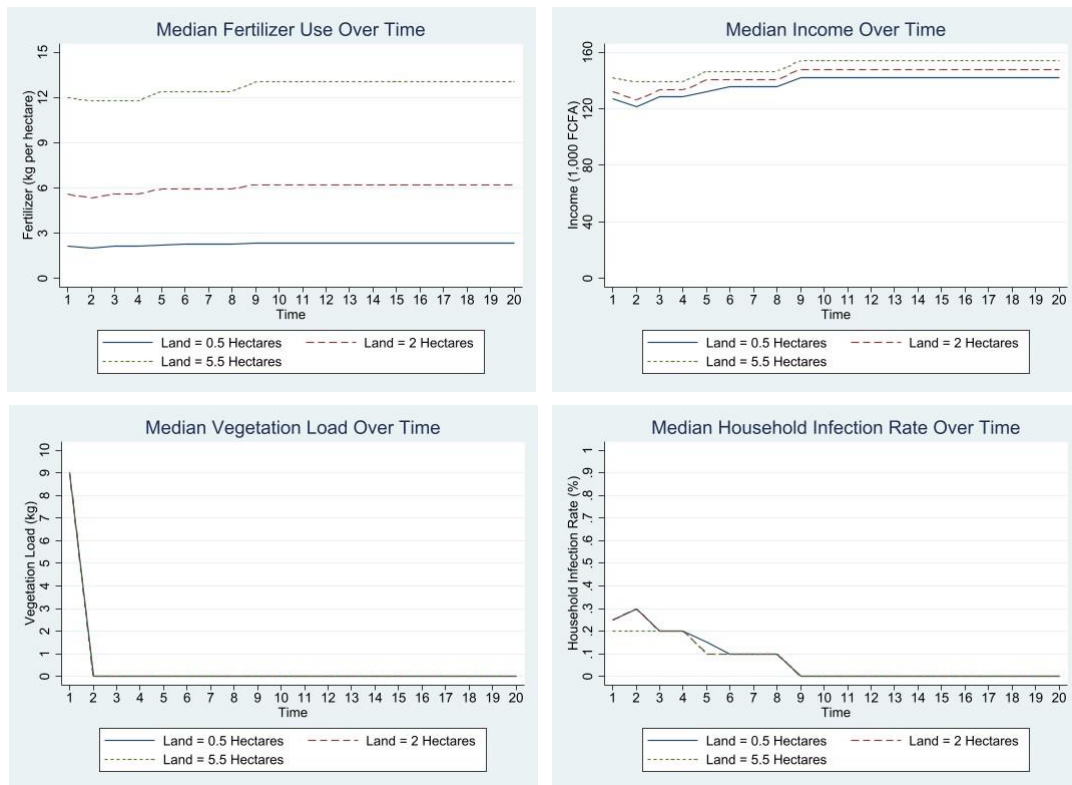
As with the previous case, in this scenario for all household types, households allocate a very small fraction of their labor to vegetation harvest (Figure 4.5). In this setting households fully clear the water source within the first period, completely eliminating the *Ceratophyllum* population so there is no possibility of vegetation regrowth (Figure 6). Households still use fertilizer on their plots (Figure 4.6), but now, by assumption, fertilizer use does not spur new vegetation growth. We see the corresponding fall in infection and rise in labor availability. Infection persists for a bit longer because deworming is sporadic and it takes time for every infected member of the household to receive a deworming draw (Figures 4.5 and 4.6). Incomes rise significantly with the increase in labor availability, demonstrating that vegetation removal has the potential to allow to break the poverty-disease trap (Figure 4.6). In both cases with vegetation harvest, the returns to compost in food production are large enough to induce take-up of vegetation harvest. However, fully eliminating infection and breaking free of the poverty-disease trap requires that households fully clear the water source of all vegetation, which is tricky when fertilizer use spurs more vegetation growth.

Figure 4.5: Median Labor Availability and Labor Allocation Shares for Simulations with Vegetation Harvest and No Fertilizer Effect



Notes: The top left plots the median labor availability (the labor endowment scaled based on realized infections) across 100 20-year simulations for three different household land endowments. The top right reports the median food labor share, the bottom left reports the median leisure share and the bottom right reports the median vegetation harvest labor share. Medians are within each land endowment and within each time period across the 100 simulations. Household size is 10, so the maximum labor availability is 10.

Figure 4.6: Median Fertilizer Use, Income, Household Infection Rate, and Vegetation Load for Simulations with Vegetation Harvest and No Fertilizer Effect



Notes: The top left plots the median fertilizer use in kgs per hectare across 100 20-year simulations for three different household land endowments. The top right reports the median income in 1,000s of FCFA, the bottom left reports the median vegetation load (population) in the water source in kgs and the bottom right reports the median household infection rate. Medians are within each land endowment and within each time period across the 100 simulations. Aquatic vegetation load represents the size of the snail habitat within the village water access point used by the household. The infection rate of the household is the number of infected individuals divided by total number of household members (the number infected plus the number not infected).

CHAPTER 5

DISCUSSION AND CONCLUSION

We develop a micro-founded model of a poverty-disease trap by linking a non-separable agricultural household model to one of schistosomiasis disease ecology through household labor availability, labor allocation choices, and optimal fertilizer use. We find evidence of a poverty-disease trap when we consider the status quo without aquatic vegetation harvest, wherein infection prevalence is consistently high and the household's labor availability and thus income are steadily low. When we allow for vegetation harvest, we see lower infection levels and higher incomes. But the role of household fertilizer use as a mechanism behind the poverty-disease trap becomes clearer. Rapid vegetation regrowth prohibits households from fully clearing the water source, so infection remains, albeit at a lower level than in the status quo case. Eliminating the vegetation growth spurred by household fertilizer use, allows the household to fully rid the water source of aquatic vegetation. Without any snail habitat, schistosomiasis infection drops to zero and households are able to use their full labor endowment raising incomes, and breaking household's out of the poverty-disease trap. Thus, vegetation harvest has the potential to allow households to break free of the cycle of schistosomiasis infection and reinfection but only in combination with measures that reduce nutrient runoff that spurs vegetation regrowth or allowing for more frequent vegetation cleaning.

One key limitation of our modeling strategy is how vegetation harvest limits impact the household's ability to fully clear the water source. Because the household solves for the optimal amount of vegetation harvest based on the current level of

vegetation in the system and then we add any growth spurred by fertilizer, the current model does not allow households to harvest any of the vegetation growth caused by fertilizer. Therefore, it would be possible for households to fully clear the water source if they were allowed to harvest more vegetation than the current static limit or if they were able to harvest vegetation at multiple time periods throughout the year. The current model only allows households to remove vegetation once annually. More frequent efforts would limit vegetation regrowth and the level of vegetation could drop even when we do allow for fertilizer effects on vegetation. The annual timestep on the household model is more tractable to study how households make decisions over an agricultural season. We know, however, that households continually update their optimal labor allocation (Fafchamps, 1993; Dillon, 2017) and could clear vegetation more frequently than allowed by the current model. While our model abstracts away from these points, we can clearly reveal mechanisms and prospective intervention points. Our results highlight the importance of keeping water access points free of aquatic vegetation that provides habitat to snails, the intermediate vector of schistosomiasis. When aquatic vegetation grows within water access points, it becomes difficult to break out of the poverty-disease trap.

Additionally, our model only currently explores the representative household's choices, but these water sources and water access points serve many households at one time. In the case of fertilizer use, one household's decision to use lots of fertilizer will spill over into the common water source increasing the vegetation population for all households who use that water source. This provides an opportunity for households to harvest more vegetation if they would like, but it also poses a greater risk to them

because they now face more vegetation and a higher infection prevalence due to others' decisions in the village. A natural extension of the current model would build out these interactions into a model of a small community to trace out the spillovers within the village. Our results document the sizeable effect small levels of fertilizer runoff can have on the system, thus documenting these village externalities may prove helpful to fully understanding and tackling the poverty-disease trap.

While this model focuses on the specific context of the Saint Louis and Louga regions in Senegal, the principles of the interventions apply to all settings where schistosomiasis is endemic. *Ceratophyllum*, the keystone aquatic vegetation species of interest in the model, is found throughout Africa and on every continent with endemic schistosomiasis (Haggerty et al., 2020). Therefore, the model of vegetation removal can be applied to settings throughout the developing world and has the potential to benefit millions that are suffering from schistosomiasis infection. Furthermore, Gao et al. (2011) report that targeting snails, as is the case with aquatic vegetation removal, is the most effective way to reduce schistosomiasis transmission. Thus, we identify and model a key potential channel to reduce disease burdens. Finally, this model highlights the importance of understanding feedback loops between household economic decision making and the environment, which has applications to other neglected tropical diseases, but also to thinking about how households and environments may co-evolve in response to climate change. Therefore, we see this model as a general framework to thinking about the relationship between human and environmental systems.

Overall, we document the existence of a poverty-disease trap caused by schistosomiasis infection in northern Senegal. We can tackle infection via a novel intervention, aquatic vegetation removal, which disrupts the infection cycle instead of relying on mass deworming events to clear human infections. By clearing the waterways, households reduce their own infection risk. Other work in Kenya finds significant impacts of deworming on child learning and that of their siblings (Miguel & Kremer, 2004; Ozier, 2018) and labor market outcomes later in life after deworming (Baird et al., 2016; Hamory et al., 2021). Thus, there are large potential long-term benefits of aquatic vegetation removal not modeled nor discussed here. Because of its widespread prevalence, policy makers should consider aquatic vegetation removal and other forms of schistosomiasis infection control as key public health interventions that greatly increase the quality of life for millions of people.

APPENDIX A

HARVESTED VEGETATION PRODUCTION

We use experimental field trial data collected from Rohr et al. (2022) on the amount of vegetation removed and the number of labor days devoted to harvesting vegetation to estimate the parameters in the production function of harvested vegetation (Equation 19). We estimate the harvested vegetation production

$$\ln(\text{Kg of harvested vegetation})_i = \alpha + \beta \ln(\text{person days})_i + \varepsilon_i \quad (27)$$

The coefficient estimate β is our direct estimate of γ_1 in Equation 19 and we calculate β_v from the estimate of the constant α using $\beta_v = \exp(\alpha)$. Results from the estimation are reported in Table A.1.

Table A.1: Vegetation Production Function Estimates

	Log(kg of vegetation)
Log(person days)	0.260*** (0.0581)
Constant	2.674*** (0.141)
N	92
Adj. R ²	0.208

Notes: Robust standard errors in parentheses. * p < 0.1, ** p < 0.05, *** p < 0.01

APPENDIX B

DISEASE ECOLOGY SUBMODEL PARAMETERIZATION

We base the disease ecology submodel on Gao et al. (2011). We use experimental estimates of parameters in the local population in Senegal from Nguyen et al. (2021) as a guide to adjust model parameters to match human infection levels observed within the region. Table B.1 reports and describes the starting parameters we used to simulate the model. We excluded human births and deaths from this simulation.¹¹

The continuous time equations are:

Susceptible snails:

$$\frac{dS_2}{dt} = \Lambda_2 - \frac{\beta_2 M S_2}{M_0 + \epsilon M^2} - \mu_2 S_2 \quad (28)$$

Infected snails:

$$\frac{dI_2}{dt} = \frac{\beta_2 M S_2}{M_0 + \epsilon M^2} - (\mu_2 + \delta_2) I_2 \quad (29)$$

Cercariae:

$$\frac{dP}{dt} = \lambda_2 I_2 - \mu_4 P \quad (30)$$

Susceptible Humans:

$$\frac{dS_1}{dt} = -\frac{\beta_1 P S_1}{1 + \alpha_1 P} + \eta I_1 \quad (31)$$

Infected Humans:

¹¹ Over a relatively short time horizon, 20 years or less, assuming away human population growth or decline for an individual family is reasonable as it represents roughly one generation.

$$\frac{dI_1}{dt} = \frac{\beta_1 P S_1}{1 + \alpha_1 P} - \eta I_1 \quad (32)$$

Miracidia:

$$\frac{dM}{dt} = k \lambda_1 I_1 - \mu_3 M \quad (33)$$

Table B.1: Parameters for the Disease Ecology Model in Gao et al. (2011)

Parameter	Description	Value
Λ_2	Snail recruitment rate	200 d ⁻¹
β_1	Contact between cercariae and humans	0.406×10^{-8}
β_2	Probability of snail infection from miracidia	0.615
μ_2	Snail natural mortality rate	0.000569
μ_3	Miracidial mortality rate	0.9
μ_4	Cercarial mortality rate	0.004
δ_2	Snail death rate from infection	0.0004012
λ_1	Hatching rate of miracidia	0.00232
λ_2	Cercarial emergence rate	2.6
α_1	Saturation coefficient for cercarial infectivity	0.3×10^{-8}
M_0	Contact rate between miracidia and snails	1.00×10^6
ϵ	Saturation coefficient for miracidial infectivity	0.30
k	Eggs released per infected human	300
η	Treatment rate of infected humans	0.00068

B.1 Modifications

We calibrated the human population to match the household-level analysis in the Senegalese context. The household size is set at 10 where 7.5 humans start as susceptible and 2.5 are infected, matching the 25% baseline prevalence of *S. mansoni* in the region reported by Rohr et al. (2022). Modifications to the original model

parameters reported in Gao et al. (2011) are required because we significantly reduce the size of the human population and eliminate human births and deaths to integrate the disease ecology model of schistosomiasis with an economic model of agricultural households.

We start with the parameters in Gao et al. (2011) and then calibrate the model from these parameter starting points with the goal of finding a steady state at or very close to 25% infection with 10 humans in the model (so 7.5 susceptible humans and 2.5 infected humans). We calibrate the parameters to achieve population stability in the snails and then increase infection until the human infection stabilized near 25%.

Finally, we added vegetation into the model. We use a general logistic growth function for vegetation, where r is the growth rate, and K is the carrying capacity. The carrying capacity was estimated from vegetation data (Rohr et al., 2022). We chose the growth rate to match rapid regrowth consistent with rates observed at study sites in Rohr et al. (2022). The logistic growth function is reported below:

$$\frac{dN}{dt} = r \times N \times \left(1 - \frac{N}{K}\right) \quad (34)$$

To connect vegetation to the existing system, a parameter χ is added to the snails' population equations. For every kilogram of vegetation below the carrying capacity, the snail population is reduced by χ percent. We start the vegetation population at the carrying capacity and thus vegetation has no effect on the other populations in these model runs. Table B.2 reports all starting values and adjusted parameters.

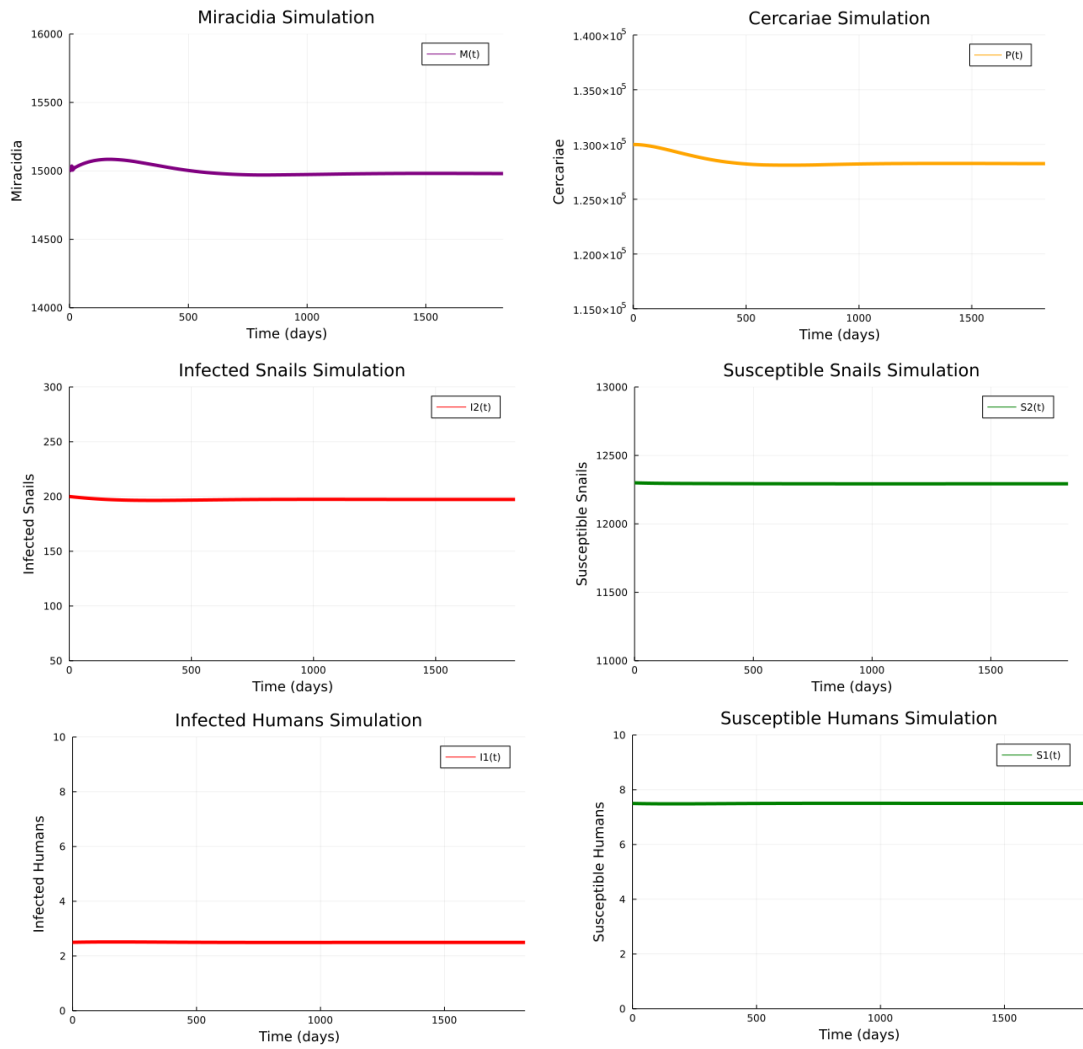
Table B.2: Adjusted Parameters for the Disease Ecology Model

Parameter	Description	Value	Modification
r	Vegetation growth rate	0.05	Yes
K	Vegetation carrying capacity	9.007 kg	Yes
ρ	Effect of fertilizer on vegetation growth	0.1	Yes
Λ_2	Snail recruitment rate	100	Yes
β_1	Contact between cercariae and humans	1.766×10^{-8}	Yes
β_2	Probability of snail infection from miracidia	0.615	No
μ_2	Snail natural mortality rate	0.008	Yes
μ_3	Miracidial mortality rate	2.5	Yes
μ_4	Cercarial mortality rate	0.004	No
δ_2	Snail death rate from infection	0.0004012	Yes
λ_1	Hatching rate of miracidia	50	Yes
λ_2	Cercarial emergence rate	2.6	No
α_1	Saturation coefficient for cercarial infectivity	0.8×10^{-8}	Yes
M_0	Contact rate between miracidia and snails	1.00×10^6	No
ϵ	Saturation coefficient for miracidial infectivity	0.30	No
χ	Snail death rate from vegetation removal	0.02842	Yes
k	Eggs released per infected human	300	No
η	Treatment rate of infected humans	0.00068	No

B.2 Simulations

Results from the simulations for each of key populations can be found in Figure B.1. We present five-year models of simulations without vegetation to confirm we have found a steady state within the disease ecology submodel. Since the vegetation population is started at the steady state level, it does not affect how the rest of the model operates and thus is not needed in these extra simulations to confirm the snails, humans, miracidia, and cercariae populations approach a steady state.

Figure B.1: Five-Year Continuous Time Simulation Results



BIBLIOGRAPHY

- ANSD. (2018). *Bulletin Mensuel des Statistiques Economiques*. Agence National de la Statistique et de la Démographie de la République du Sénégal.
http://www.ansd.sn/index.php?option=com_ansd&view=titrepublication&id=9&Itemid=287
- Baird, S., Hicks, J. H., Kremer, M., & Miguel, E. (2016). Worms at work: Long-run impacts of a child health investment. *The Quarterly Journal of Economics*, *131*(4), 1637-1680.
- Barrett, C. B., & Arcese, P. (1998). Wildlife harvest in integrated conservation and development projects: Linking harvest to household demand, agricultural production, and environmental shocks in the Serengeti. *Land Economics*, 449–465.
- Barrett, C. B., & Bevis, L. E. (2015). The self-reinforcing feedback between low soil fertility and chronic poverty. *Nature Geoscience*, *8*(12), 907–912.
- Barrett, C. B., & Carter, M. R. (2013). The economics of poverty traps and persistent poverty: Empirical and policy implications. *Journal of Development Studies*, *49*(7), 976–990.
- Barrett, C. B., Carter, M. R., & Chavas, J.-P. (2019). *The Economics of Poverty Traps*. University of Chicago Press Chicago.
- Barrett, C. B., Garg, T., & McBride, L. (2016). Well-being dynamics and poverty traps. *Annual Review of Resource Economics*, *8*, 303–327.
- Barrett, C. B., Marenya, P. P., McPeak, J., Minten, B., Murithi, F., Oluoch-Kosura, W., Place, F., Randrianarisoa, J. C., Rasambainarivo, J., & Wangila, J. (2006).

- Welfare dynamics in rural Kenya and Madagascar. *Journal of Development Studies*, 42(2), 248–277.
- Barrett, C. B., & Swallow, B. M. (2006). Fractal poverty traps. *World Development*, 34(1), 1–15.
- Berthélemy, J.-C., Thuilliez, J., Doumbo, O., & Gaudart, J. (2013). Malaria and protective behaviours: Is there a malaria trap? *Malaria Journal*, 12(1), 1–9.
- Bliss, C. & Stern, N. (1978). Productivity, wages, and nutrition. *Journal of Development Economics*, 5, 331-362.
- Bonds, M. H., Keenan, D. C., Rohani, P., & Sachs, J. D. (2010). Poverty trap formed by the ecology of infectious diseases. *Proceedings of the Royal Society B: Biological Sciences*, 277(1685), 1185–1192.
- Carter, M. R., & Barrett, C. B. (2006). The economics of poverty traps and persistent poverty: An asset-based approach. *Journal of Development Studies*, 42(2), 178–199.
- DAPSA. (2017). *Enquête agricole annuelle (AEE), 2017/2018, Direction de l'Analyse, de la Prévision et des Statistiques agricoles (DAPSA) de la République du Sénégal*. www.dapsa.gouv.sn
- Dasgupta, P. (1993). *An Inquiry into Well-Being and Destitution*. Oxford University Press Oxford.
- Dasgupta, P. (1997). Nutritional status, the capacity for work, and poverty traps. *Journal of Econometrics* 77(1), 5-37.
- Dasgupta, P. & Ray, D. (1986). Inequality as a determinant of malnutrition and unemployment: Theory. *The Economic Journal*, 96(384), 1011-1034.

- Dasgupta, P. & Ray, D. (1987). Inequality as a determinant of malnutrition and unemployment: Policy. *The Economic Journal*, 97(385), 177-188.
- Dillon, B. (2017). Private Information and Dynamic Risk. *Working Paper*.
- Fafchamps, M. (1993). Sequential labor decisions under uncertainty: An estimable household model of west-African farmers. *Econometrica*, 61(5), 1173-1197.
- Foster, A. D., & Rosenzweig, M. R. (1994). A test for moral hazard in the labor market: Contractual arrangements, effort, and health. *Review of Economics and Statistics*, 213–227.
- Gao, S., Liu, Y., Luo, Y., & Xie, D. (2011). Control problems of a mathematical model for schistosomiasis transmission dynamics. *Nonlinear Dynamics*, 63(3), 503–512.
- Garchitorena, A., Ngonghala, C. N., Guegan, J.-F., Texier, G., Bellanger, M., Bonds, M., & Roche, B. (2015). Economic inequality caused by feedbacks between poverty and the dynamics of a rare tropical disease: The case of Buruli ulcer in sub-Saharan Africa. *Proceedings of the Royal Society B: Biological Sciences*, 282(1818), 20151426.
- Goenka, A., & Liu, L. (2020). Infectious diseases, human capital and economic growth. *Economic Theory*, 70(1), 1–47.
- Grimes, J. E., Croll, D., Harrison, W. E., Utzinger, J., Freeman, M. C., & Templeton, M. R. (2015). The roles of water, sanitation and hygiene in reducing schistosomiasis: A review. *Parasites & Vectors*, 8(1), 1–16.
- Gryseels, B., Polman, K., Clerinx, J., & Kestens, L. (2006). Human schistosomiasis. *The Lancet*, 368(9541), 1106–1118.

- Haggerty, C. J., Bakhoun, S., Civitello, D. J., De Leo, G. A., Jouanard, N., Ndione, R. A., Remais, J. V., Riveau, G., Senghor, S., Sokolow, S. H., Sow, S., Wole, C., Wood, C., Jones, I., Chamberlin, A. J., & Rohr, J. R. (2020). Aquatic macrophytes and macroinvertebrate predators affect densities of snail hosts and local production of schistosome cercariae that cause human schistosomiasis. *PLoS Neglected Tropical Diseases*, *14*(7), e0008417.
- Halstead, N. T., Hoover, C. M., Arakala, A., Civitello, D. J., De Leo, G. A., Gambhir, M., Johnson, S. A., Jouanard, N., Loerns, K. A., McMahon, T. A., Ndione, R. A., Nguyen, K., Raffel, T. R., Remais, J. V., Riveau, G., Sokolow, S. H., & Rohr, J. R. (2018). Agrochemicals increase risk of human schistosomiasis by supporting higher densities of intermediate hosts. *Nature Communications*, *9*(1), 1–10.
- Hamory, J., Miguel, E., Walker, M., Kremer, M., & Baird, S. (2021). Twenty-year economic impacts of deworming. *Proceedings of the National Academy of Sciences*, *118*(14), e2023185118.
- Hoover, C. M., Rumschlag, S. L., Strgar, L., Arakala, A., Gambhir, M., De Leo, G. A., Sokolow, S. H., Rohr, J. R., & Remais, J. V. (2020). Effects of agrochemical pollution on schistosomiasis transmission: A systematic review and modelling analysis. *The Lancet Planetary Health*, *4*(7), e280–e291.
- Hoover, C. M., Sokolow, S. H., Kemp, J., Sanchirico, J. N., Lund, A. J., Jones, I., Higginson, T., Riveau, G., Savaya, A., Coyle, S., Wood, C. L., Micheli, F., Casagrandi, R., Mari, L., Gatto, M., Rinaldo, A., Perez-Saez, J., Rohr, J. R., Sagi, A., Remais, J. V., & De Leo, G. A. (2020). Modelled effects of proawn

aquaculture on poverty alleviation and schistosomiasis control. *Nature Sustainability* 2(7), 611-620.

Hotez, P. J., Alvarado, M., Basáñez, M.-G., Bolliger, I., Bourne, R., Boussinesq, M., Brooker, S. J., Brown, A. S., Buckle, G., Budke, C. M., Carabin, H., Coffeng, L. E., Fèvre, E. M., Fürst, T., Halasa, Y. A., Jasrasaria, R., Johns, N. E., Keiser, J., King, C. H., Lozano, R., Murdoch, M. E., O’Hanlon, S., Pinon, S. D. S., Pullman, R. L., Ramaiah, K. D., Roberts, T., Shepard, D. S., Smith, J. L., Stolk, W. A., Undurraga, E. A., Utzinger, J., Wang, M., Murray, C. J. L., & Naghavi, M. (2014). The global burden of disease study 2010: Interpretation and implications for the neglected tropical diseases. *PLoS Neglected Tropical Diseases*, 8(7), e2865.

King, C. H., Dickman, K., & Tisch, D. J. (2005). Reassessment of the cost of chronic helminthic infection: A meta-analysis of disability-related outcomes in endemic schistosomiasis. *The Lancet*, 365(9470), 1561–1569.

Kjetland, E. F., Ndhlovu, P. D., Gomo, E., Mduluzza, T., Midzi, N., Gwanzura, L., Mason, P. R., Sandvik, L., Friis, H., & Gundersen, S. G. (2006). Association between genital schistosomiasis and HIV in rural Zimbabwean women. *AIDS*, 20(4), 593–600.

Kraay, A., & McKenzie, D. (2014). Do poverty traps exist? Assessing the evidence. *Journal of Economic Perspectives*, 28(3), 127–148.

Léger, E., Borlase, A., Fall, C. B., Diouf, N. D., Diop, S. D., Yasenev, L., Catalano, S., Thiam, C. T., Ndiaye, A., Emery, A., Morrell, A., Rabone, M., Ndao, M., Faye, B., Rollinson, D., Rudge, J. W., Sène, M., & Webster, J. P. (2020).

- Prevalence and distribution of schistosomiasis in human, livestock, and snail populations in northern Senegal: A One Health epidemiological study of a multi-host system. *The Lancet Planetary Health*, 4(8), e330–e342.
- Liang, S., Abe, E. M., & Zhou, X.-N. (2018). Integrating ecological approaches to interrupt schistosomiasis transmission: Opportunities and challenges. *Infectious Diseases of Poverty*, 7(1), 1–6.
- Liberatos, J. D. (1987). *Schistosoma mansoni*: Male-based sex ratios in snails and mice. *Experimental Parasitology*, 64(2), 165-177.
- Lund, A. J., Rehkopf, D. H., Sokolow, S. H., Sam, M. M., Jouanard, N., Schacht, A.-M., Senghor, S., Fall, A., Riveau, G., De Leo, G. A., & Lopez-Carr, D. (2021). Land use impacts on parasitic infection: A cross-sectional epidemiological study on the role of irrigated agriculture in schistosome infection in a dammed landscape. *Infectious Diseases of Poverty*, 10(1), 1–10.
- Lybbert, T. J., Barrett, C. B., Desta, S., & Layne Coppock, D. (2004). Stochastic wealth dynamics and risk management among a poor population. *Economic Journal*, 114(498), 750–777.
- Lybbert, T. J., Just, D. R., & Barrett, C. B. (2013). Estimating risk preferences in the presence of bifurcated wealth dynamics: Can we identify static risk aversion amidst dynamic risk responses? *European Review of Agricultural Economics*, 40(2), 361–377.
- McCullough, E. B. (2017). Labor productivity and employment gaps in Sub-Saharan Africa. *Food Policy*, 67, 133–152.
- Miguel, E., & Kremer, M. (2004). Worms: Identifying impacts on education and

- health in the presence of treatment externalities. *Econometrica*, 72(1), 159–217.
- Mohammed, A. Z., Edino, S. T., & Samaila, A. A. (2007). Surgical pathology of schistosomiasis. *Journal of the National Medical Association*, 99(5), 570.
- Ngonghala, C. N., De Leo, G. A., Pascual, M. M., Keenan, D. C., Dobson, A. P., & Bonds, M. H. (2017). General ecological models for human subsistence, health and poverty. *Nature Ecology & Evolution*, 1(8), 1153–1159.
- Ngonghala, C. N., Pluciński, M. M., Murray, M. B., Farmer, P. E., Barrett, C. B., Keenan, D. C., & Bonds, M. H. (2014). Poverty, disease, and the ecology of complex systems. *PLoS Biology*, 12(4), e1001827.
- Nguyen, K. H., Boersch-Supan, P. H., Hartman, R. B., Mendiola, S. Y., Harwood, V. J., Civitello, D. J., & Rohr, J. R. (2021). Interventions can shift the thermal optimum for parasitic disease transmission. *Proceedings of the National Academy of Sciences*, 118(11).
- Ozier, O. (2018). Exploiting externalities to estimate the long-term effects of early childhood deworming. *American Economic Journal: Applied Economics*, 10(3), 235–262.
- Pitt, M. M., Rosenzweig, M. R., & Hassan, M. N. (1990). Productivity, health, and inequality in the intrahousehold distribution of food in low-income countries. *American Economic Review*, 1139–1156.
- Pluciński, M. M., Ngonghala, C. N., & Bonds, M. H. (2011). Health safety nets can break cycles of poverty and disease: A stochastic ecological model. *Journal of the Royal Society Interface*, 8(65), 1796–1803.

- Pluciński, M. M., Ngonghala, C. N., Getz, W. M., & Bonds, M. H. (2013). Clusters of poverty and disease emerge from feedbacks on an epidemiological network. *Journal of The Royal Society Interface*, *10*(80), 20120656.
- Ray, D. & Streufert, P. (1993). Dynamic equilibria with unemployment due to undernourishment. *Economic Theory*, *3*(1), 61-85.
- Rohr, J. R., Bakhoun, S., Barrett, C. B., Chamberlin, A. J., Civitello, D. J., Doruska, M. J., De Leo, G. A., Haggerty, C. J. E., Jones, I., Jouanard, N., Ly, A. T., Ndione, R. A., Remais, J. V., Riveau, G., Sack, A., Schacht, A.-M., Senghor, S., Sokolow, S. H., & Wolfe, C. (2022). A planetary health solution for disease, sustainability, food, water, and poverty challenges. *MedRxiv*.
<https://doi.org/10.1101/2022.08.02.22278196>
- Rohr, J. R., Barrett, C. B., Civitello, D. J., Craft, M. E., Delius, B., DeLeo, G. A., Hudson, P. J., Jouanard, N., Nguyen, K. H., Ostfeld, R. S., Remais, J. V., Riveau, G., Sokolow, S. H., & Tilman, D. (2019). Emerging human infectious diseases and the links to global food production. *Nature Sustainability*, *2*(6), 445–456.
- Şevik, F., Tosun, İ., & Ekinçi, K. (2018). The effect of FAS and C/N ratios on co-composting of sewage sludge, dairy manure and tomato stalks. *Waste Management*, *80*, 450-456.
- Singh, I., Squire, L., & Strauss, J. (1986). *Agricultural Household Models: Extensions, Applications, and Policy*. The World Bank.
- Steinmann, P., Keiser, J., Bos, R., Tanner, M., & Utzinger, J. (2006). Schistosomiasis and water resources development: Systematic review, meta-analysis, and

- estimates of people at risk. *The Lancet Infectious Diseases*, 6(7), 411–425.
- Stelma, F., Talla, I., Verle, P., Niang, M., & Gryseels, B. (1994). Morbidity due to heavy *Schistosoma mansoni* infections in a recently established focus in northern Senegal. *American Journal of Tropical Medicine and Hygiene*, 50(5), 575–579.
- Stephens, E. C., Nicholson, C. F., Brown, D. R., Parsons, D., Barrett, C. B., Lehmann, J., Mbugua, D., Ngoze, S., Pell, A. N., & Riha, S. J. (2012). Modeling the impact of natural resource-based poverty traps on food security in Kenya: The Crops, Livestock and Soils in Smallholder Economic Systems (CLASSES) model. *Food Security*, 4(3), 423–439.
- Stiglitz, J. E. (1976). The efficiency wage hypothesis, surplus labour, and the distribution of income in LDCs. *Oxford Economic Papers*, 28(2), 185–207.
- Toth, R. (2015). Traps and thresholds in pastoralist mobility. *American Journal of Agricultural Economics*, 97(1), 315–332.
- Varis, O., Stucki, V., & Fraboulet-Jussila, S. (2006). The Senegal River Case. *Soil & Water*, 1–10.
- Verjee, M. A. (2019). Schistosomiasis: Still a cause of significant morbidity and mortality. *Research and Reports in Tropical Medicine*, 10, 153.
- Vollset, E. S., Goren, E., Yuan, C.-W., Cao, J., Smith, A. E., Hsiao, T., Bisignano, C., Azhar, G. S., Castro, E., Chaleck, J., Dolger, A. J., Frank, T., Fukutaki, K., Hay, S. I., Lozano, R., Mokdad, A. H., Nandakumar, V., Pierce, M., Pletcher, M., Robalik, T., Steuben, K. M., Wunrow, H. Y., Zlavog, B. S., & Murray, C. L. (2020). Fertility, mortality, migration, and population scenarios for 195

countries and territories from 2017 to 2100: A forecasting analysis for the Global Burden of Disease Study. *The Lancet*, 396(10258), 1285-1306.

WAEMU Commission. (2018). *Harmonized Survey on Households Living Standards, Senegal 2018-2019. Ref. SEN_2018_EHCVM_v02_M*. Dataset downloaded from www.microdata.worldbank.org on September 23, 2022.

Zimmerman, F. J., & Carter, M. R. (2003). Asset smoothing, consumption smoothing and the reproduction of inequality under risk and subsistence constraints. *Journal of Development Economics*, 71(2), 233–260.